A novel therapeutic peptide targeting myocardial reperfusion injury

Prisca Boisguerin, Aurélie Covinhes, Laura Gallot, Christian Barrère, Anne Vincent, Muriel Busson, Christophe Piot, Joël Nargeot, Bernard Lebleu, Stéphanie Barrère-Lemaire

A novel therapeutic peptide targeting myocardial reperfusion injury.

Prisca Boisguérin[1,6], Aurélie Covinhes[2,3], Laura Gallot[2,3], Christian Barrère[2,3], Anne Vincent[2,3], Muriel Busson[4], Christophe Piot[2,3,5], Joël Nargeot[2,3], Bernard Lebleu[6], Stéphanie Barrère-Lemaire[2,3*]

[1], CRBM, Université de Montpellier, CNRS, Montpellier, France;

[2], IGF, Université de Montpellier, CNRS, INSERM, Montpellier, France;

[3], Laboratory of Excellence Ion Channel Science and Therapeutics, Valbonne, France;

[4], IRCM, Université de Montpellier, INSERM, Montpellier, France;

[5], Département de Cardiologie Interventionnelle, Clinique du Millénaire, Montpellier, France;

[6], DIMNP, Université de Montpellier, CNRS, Montpellier, France.

[*] **Corresponding author:**

Stéphanie Barrère-Lemaire

Institut de Génomique Fonctionnelle

141, rue de la Cardonille - 34094 Montpellier Cedex 5 - France

Tel: +33 4 34 35 92 46 - Fax: +33 4 67 54 24 32

Email: stephanie.barrere@igf.cnrs.fr

Original article

7268 words

Abstract

Aims

Regulated cell death is a main contributor of myocardial ischemia-reperfusion injury during acute myocardial infarction. In this context, targeting apoptosis could be a potent therapeutical strategy. In a previous study, we showed that DAXX (death-associated protein) was essential for transducing the FAS-dependent apoptotic signal during IR injury. The present study aims at evaluating the cardioprotective effects of a synthetic peptide inhibiting FAS:DAXX interaction.

Methods and results

An interfering peptide was engineered and then coupled to the Tat cell penetrating peptide (Tat-DAXXp). Its internalization and anti-apoptotic properties were demonstrated in primary cardiomyocytes. Importantly, an intravenous bolus injection of Tat-DAXXp (1 mg/kg) 5 min before reperfusion in a murine myocardial ischemia-reperfusion model decreased infarct size by 48% after 24 h of reperfusion. In addition, Tat-DAXXp was still efficient after a 30-min delayed administration, and was completely degraded and eliminated within 24 h thereby reducing risks of potential side effects. Importantly, Tat-DAXXp reduced mouse early post-infarction mortality by 67%. Mechanistically, cardioprotection was supported by both anti-apoptotic and pro-survival effects, and an improvement of myocardial functional recovery as evidenced in *ex vivo* experiments.

Conclusions

Our study demonstrates that a single dose of Tat-DAXXp injected intravenously at the onset of reperfusion leads to a strong cardioprotection *in vivo* by inhibiting ischemia-reperfusion injury validating Tat-DAXXp as a promising candidate for therapeutic application.

Translational Perspective

Our study proposes a peptidic strategy targeting apoptosis far upstream in the FAS receptor signalling cascade for limiting reperfusion injury in AMI patients. This new approach displays features required for clinical applications.

A single injection of the therapeutic peptide could be associated with both thrombolysis or at reperfusion during primary coronary angioplasty with possible delayed application, which would open new perspectives in clinical setting for the management of myocardial infarction.

1. Introduction

Prompt reperfusion after acute myocardial infarction (AMI) using thrombolysis or primary coronary angioplasty has improved functional myocardial recovery and increased patient survival dramatically.[1, 2] Unfortunately, reperfusion also induces lethal injuries adding on those related to prolonged ischemia. These are partly linked to the activation of regulated cell death cascades upon abrupt restoration of oxygen supply. Lethal reperfusion injury results from death of cardiac cells that were viable at the end of the ischemic period before myocardial reperfusion.[3, 4] Targeting regulated cell death pathways after an ischemic event appeared as a promising and innovative therapeutic strategy to prevent reperfusion injury and to limit infarct size.[5-7] Although several drugs targeting the mitochondrial intrinsic pathway have shown cardioprotective effects in animal models they all failed to be efficient in clinical trials.[8, 9]

The death associated protein DAXX (*Death-domain associated protein-6*; 120 kDa - 740 amino acids) appears to play a key role in ischemia-reperfusion (IR) injury in various organs including the heart. The DAXX protein plays different roles depending of its subcellular localization. Indeed, nuclear DAXX is reported to regulate transcription acting mainly as an anti-apoptotic contributor.[10] Upon cytosolic relocalization after ischemic and oxidative stress, this same protein acquires a pro-apoptotic role.[11, 12] Upon the *Apoptosis signal-regulating kinase 1* (ASK1)-shuttling, DAXX interacts with the intracellular region of the *First Apoptosis Signal* (FAS) death-receptor pathway and triggers the downstream apoptotic signalling pathway.[13] Therefore, we have focused on the development of therapeutic tools targeting the FAS:DAXX interaction as a new treatment for AMI patients.

Since protein:protein interactions are promoted by large surfaces lacking well-defined binding pockets, a peptidic strategy appeared appropriate to uncouple the FAS:DAXX interaction. The designed interfering peptide DAXXp was coupled to the Tat cell penetrating

peptide (CPP) to allow efficient cellular internalization.[14] Tat was selected among various available CPPs since it was previously used successfully to deliver different molecules in cardiac tissues to reduce myocardial IR injury.[5, 15-17]

Our study was designed to (i) evaluate the internalization and anti-apoptotic activity of Tat-DAXXp (TD) *in vitro*, (ii) investigate its cardioprotective effect in a murine IR model *ex vivo* and *in vivo* and (iii) define the time window of TD administration post reperfusion *in vivo*. Altogether our results evidence the TD peptide as a promising candidate for therapeutic application during myocardial reperfusion injury.

2. Methods

See details in supplementary material online.

2.1. Peptide synthesis, peptide-array binding studies and peptide stability assays

Tat, DAXXp, Tat-DAXXp (TD), Tat-scrDAXXp (TDS) as well as the deriving sequences (see **Table S1**) were synthesized on resin by conventional Fmoc-chemistry (by the group of Dr. Volkmer or by *Intavis AG*). Peptide libraries were generated by a MultiPep SPOTrobot (*Intavis Bioanalytical Instruments AG*) on N-modified CAPE-membranes according to the standard SPOT synthesis. Peptide stability was evaluated in the precense of 20% mouse serum by HPLC (*Waters*) at various times (0 h, 1 h, 2 h, 4 h and 8 h).

2.2. Cell cultures

Mouse myoblast cells were commercially acquired (C2C12 – ATCC: CRL-1772™).

Primary neonate cardiomyocytes were isolated from 1- to 2-day-old C57BL/6J mice (*Charles River Laboratories*) ventricles by enzymatic digestion.

Isolated adult murine cardiomyocytes were enzymatically dissociated on a Langendorff apparatus from control hearts or hearts subjected to global ischemia and reperfusion.

2.3 Animal experiments

All experiments were carried out on C57BL/6J mice (*Charles River laboratories*) in accordance with the European Communities Council directive of November 1986 and conformed to the "Guide for the Care and Use of Laboratory Animals" published by the US National Institutes of Health (NIH publication 8th Edition, 2011).

2.4. Langendorff ex vivo studies

For *ex vivo* experiments, C57Bl6 male mice were anesthetized with a first intramuscular injection of an anesthetic cocktail comprising ketamine (14 mg/kg, Imalgène®; *Merial*) and xylazine (14 mg/kg, Rompun®; *Bayer*), and by a second injection of pentobarbital (76.6 mg/kg; *Sanofi-Aventis*). The heart was excised after sternotomy, quickly cannulated through the aorta and mounted on a Langendorff system to be perfused with an oxygenated Krebs buffer and subjected to IR protocols.

2.5. Surgical protocol of myocardial ischemia/reperfusion (IR)

Investigation conformed to the 2010/63/EU Directive of the European Parliament. The surgical protocols were approved by the “Comité d’éthique pour l’expérimentation animale Languedoc-Roussillon” (CEEA-LR) with the authorization number CE-LR-0814.
Mice were anaesthetized with an intramuscular (IM) injection of ketamine (50 mg/kg), xylazine (10 mg/kg) and chlorpromazine (1.25 mg/kg; Largactil® 5 mg/ml; *Sanofi-Aventis*). After a second injection of ketamine and xylazine (same doses), a left lateral thoracotomy and a coronary artery ligature were performed.

When reperfusion lasted 60 min, a third administration of ketamine/xylazine was performed (same doses, IM) at the onset of reperfusion. For longer reperfusion (24h), mice underwent subcutaneous administration of lidocaine (1.5 mg/kg) and a postoperative awakening in an emergency care unit.

At the end of all *in vivo* protocols, mice were anesthetized with an intramuscular injection of an anaesthetic mixture comprising ketamine (50 mg/kg), xylazine (10 mg/kg) and chlorpromazine (1.25 mg/kg) and the heart was harvested for further analysis.

2.6. Infarct size assessment

Infarct size measurements were obtained after dual coloration of left ventricular sections by phtalocyanin blue dye and 2,3,5-triphenyltetrazolium chloride.

2.7. DNA fragmentation assay

DNA fragmentation was quantified *in vitro* on cell lysates and *in vivo* in transmural samples of non-ischemic or ischemic areas of left ventricle (LV). with an enzyme-linked immunosorbent assay kit (Cell Death ELISA; *Roche Diagnostics*) designed to measure of histone-complexed DNA fragments (mono- and oligonucleosomes) out of the cytoplasma of cells after the induction of apoptosis.

2.8. Immunoblotting

Western blots were performed from LV protein extracts from *ex vivo* hearts using antibodies as decribed in the supplemental materials.

2.9. Immunostaining

Fixated cells were incubated with an anti-DAXX antibody (*Santa Cruz Biotechnologies*) to evaluate endogeneous DAXX localisation after an ischemic stress. To follow TD accumulation in the LV, carboxyfluorescein labelled TD peptide was injected 5 min before the reperfusion. LV deparaffinized sections were imaged.

2.10. SPECT-CT imaging

Whole-body SPECT/CT images were acquired with a 4-head multiplexing multipinhole NanoSPECT camera (*Bioscan Inc*.) at various times (0 h, 3 h, 6 h, and 24 h) after tail vein injection of 10 MBq radiolabeled ^{125}I-Tat-DAXXp in control mice or at the time of reperfusion in IR mice.

2.11. Statistical analysis

Statistical analysis was performed only for $n \geq 5$ independent experiments. Data (mean ± SD) were analyzed with nonparametric Kruskal-Wallis test for multiple comparison or Mann-Whitney when appropriate. For repeated mesures, data were analyzed with Two-way RM ANOVA and the Tukey's or Sidak's post-test. Concerning **Figures 6B and C**, infarct size data (mean ± SD) were fitted by a linear regression model using the least squares method. Data were analyzed with GraphPad Prism 6.0 (*GraphPad Software*).

3. Results

3.1. Design of the interfering Tat-DAXXp peptide and evaluation of its cardioprotective effect in vitro.

The interfering DAXXpeptide (DAXXp) was engineered using peptide arrays generated by SPOT technology (**Figure S1**). DAXXp was coupled to the Tat CPP resulting in the Tat-DAXXp (noted TD, 3.4 kDa, 29 amino acids). Its anti-apoptotic potential and its internalization mechanism via endocytosis were first demonstrated in C2C12 murine myocytes cell line (see Supplemental Results and **Figures S2 and S3**). The minimal active sequence (MAS) of the interfering peptide was investigated resulting in the 16-mer DAXXp sequences (**Figure S4 and Table S1**), which was selected for further experiments.

In a second step, carboxyfluorescein (CF)-labelled TD internalization was confirmed in primary neonate murine cardiomyocytes by flow cytrometry (87 ± 3% of the analyzed cells) (**Figure 1A**). In contrast and as expected, the free DAXXp peptide was not internalized. As observed in C2C12 cells (**Figure S3A**), CF-TD showed first a punctuated cytosolic pattern (1 h-incubation) followed by a diffuse distribution in the cytosol at later times (4 h) (**Figure 1B**) in keeping with an endocytic uptake followed by efficient release from endocytic compartments.

The anti-apoptotic activity of TD was evaluated in primary murine cardiomyocytes submitted to an apoptotic stress (**Figure 1C**) using specific DNA fragmentation (a hallmark of apoptosis) quantification. A 44%-decrease in DNA fragmentation was observed in cardiomyocytes treated with TD ($p^*<0.05$ *versus* Tat), which was not observed with the Tat delivery vector alone or with a scrambled version (Tat-scrDAXXp, noted TDS) of the interfering peptide (**Figure 1D**), both used as controls. As expected from its poor cell uptake in this *in vitro* model, the free DAXXp did not induce any anti-apoptotic activity even at a 10 μmol/L concentration.

3.2. Effect of Tat-DAXXp on isolated perfused hearts

The protective effect of TD was evaluated on isolated perfused hearts subjected to global IR (**Figure 2A**). A significant 45%-decrease in infarct size was observed in the group of hearts reperfused with TD (p*=0.012 *versus* TDS; **Figure 2B**). TDS did not induce any cardioprotective effect compared to the control (non-treated IR).

The developed tension assessed under constant frequency stimulation during the perfusion protocol was greater in hearts perfused with TD than in those perfused with TDS or buffer alone (**Figure 2C**). Interestingly, an improvement in the coronary flow was demonstrated in the post-ischemic period in hearts treated by TD after a regional ischemia with no perturbation of the electrocardiographic (ECG) parameters (**Figure 2D**).

3.3. Evaluation of Tat-DAXXp tissue localization and degradation profile

The tissue distribution of the CF-TD construct was evaluated in the heart of mice submitted to an *in vivo* surgical protocol of myocardial infarction and injected 5 min before reperfusion (1 mg/kg). Confocal images from left ventricle (LV) slices clearly reveal cardiac cells with a green labeling indicating the peptidic presence in the cytoplasm after 1 h-reperfusion (**Figure S5A**) in agreement with the *in vitro* intracellular distribution data in primary murine cardiomyocytes (**Figure 1A**). Co-staining with DAPI showed few cases with a nuclear peptide localization (**Figure S5A**, right panel).

Metabolic stability and elimination of the peptide are critical requirement to avoid side-effects of the anti-apoptotic peptide. The peptide was rapidly degraded in a time-dependent manner in the presence of mouse serum *in vitro*, with a total degradation after 24 h (**Figure S5B**). Whole-body SPECT/CT recordings using ^{125}I-TD administration in control or IR subjected animals revealed the presence of the peptide in the heart (**Figure 3A**) and a nearly complete hepatic and renal clearance (80-100%) 24 h after its injection (**Figure 3B**).

3.4. Cardioprotective effects of the interfering peptide in vivo

Having established that the peptide was detected in the target tissue after systemic administration, we determined the optimal peptide dose for treatment in an *in vivo* IR murine model (details given in **Table S2**). Various doses of TD were administered as a single intravenous bolus 5 min before reperfusion (**Figure 3C**). After 1 h-reperfusion, a 56%-decrease in infarct size was obtained using a 1 mg/kg TD dose *versus* TDS (p**=0.006). The same efficiency was observed at a 10-fold higher dose (10 mg/kg, p>0.99). The cardioprotective effect of TD was specific to the DAXX peptide sequence since the control Tat and TDS peptides did not protect against IR injury (Tat *versus* TDS; p>0.99). In order to verify that the cardioprotection was not transient, *in vivo* experiments were performed with 24 h-reperfusion protocols. Infarct size measurements (**Table S2**) revealed a significant reduction in the presence of TD in particular at the 1 mg/kg TD dose (48% *versus* TDS; p*=0.026; **Figure 3D**). In all conditions (1 h and 24 h), there was no statistical difference between AR/LV (area at risk/left ventricle mass) among groups (**Table S2; Figure S6**). Relevant for clinical translation, a drastic 67%-decrease in mortality was observed during the critical period of 24 h post-infarction in mice treated with 1 mg/kg TD (13%, n=16) *versus* Tat (38%, n=55).

3.5. Mechanisms of cardioprotection by Tat-DAXXp

To evaluate if the cardioprotective effect of the TD peptide was correlated to a reduced apoptosis, DNA fragmentation was quantified in hearts subjected to the same *in vivo* IR 1h-reperfusion protocol. TD (1 mg/kg) inhibited apoptosis (reduction of 59% *versus* TDS; p**=0.006) while TDS did not exert any inhibitory effect *per se* (TDS *versus* Tat, p>0.99; **Figure 4A)**.

Similarly, anti-apoptotic effects of TD measured 24 h after IR were as potent than at 1h-reperfusion (reduction of 53% for TD *versus* TDS; p*=0.023), and similar to that provided by TD 10 mg/kg (TD 1 mg/kg *versus* TD 10 mg/kg, p>0.99; **Figure 4B)**. TDS did not inhibit apoptosis and did not decrease infarct size (TDS *versus* Tat, p>0.99; **Figure 4B**).

The potent anti-apoptotic effect of the TD peptide was further confirmed by Western blot analysis. In hearts subjected to IR injury, TD treatment led to a down-regulation of pJNK/JNK MAPKinase ratios and activation of caspase 3 (**Figure 4C**), FADD and cleaved caspase 8 (FAS-FADD downstream pathway, **Figure 4D**), BAD and cleaved caspase 9 (key components of mitochondria-dependent apoptosis) protein levels (**Figure 4E**). However, neither DAXX nor FAS protein levels were modified upon TD treatment compared to non-treated IR conditions (**Figures 4C** and **4D**). Finally, TD treatment did not affect necroptosis or the autophagy flux involved in IR-induced cell death[18] (**Figures S7 and S8**).

HSP70 production, a hallmark of proteotoxic stress during IR injury,[19] was also drastically decreased upon TD treatment *versus* non-treated IR conditions (**Figure 5A**). In addition, evaluation of the phosphorylation patterns of ERK1/2 and AKT pro-survival kinases, showed a significantly increased in the phosphorylation ratio in TD treated *versus* non-treated IR hearts (**Figures 5B,C)**.

Anti-apoptotic effects have been correlated to the nuclear localization of the DAXX protein.[20, 21] Thus, nuclear *versus* cytoplasmatic DAXX protein levels were measured in cells isolated from hearts subjected to IR protocol *ex vivo.* Upon IR or Tat conditions, very low levels of nuclear DAXX protein were observed and quantified compared to the Sham condition. TD treatment during reperfusion results in an increased percentage of cells with nuclear DAXX protein compared to Tat treatment (**Figures 5D and 5E)**. DAXX phosphorylation, that triggers export from the nucleus to the cytoplasm,[21] was increased upon IR and Tat treatments compared to the Sham condition (p** *versus* Sham). DAXX was

phosphorylated 1 h after TD treatment at an intermediate level between Sham and IR (p=ns *versus* IR and *versus* Sham; **Figures 5F** and **5G**) (see also Supplemental Results 2.5 and 2.6).

3.6. Therapeutic time window of Tat-DAXXp administration and elimination

In order to determine the therapeutic time window providing optimal cardioprotection, TD administration was delayed after the onset of reperfusion. Delaying peptide administration by 5, 15 or 30 min after reperfusion (see protocol **Figure 6A**) did not abolish cardioprotection in terms of infarct size or apoptosis. The protection was lost at 45 min ($TD_{\Delta 45}$ *versus* TD, p***=0.0002 for infact size and DNA fragmentation evaluated at 1 h; **Figures 6B and 6D**) consistently with our previous data on delayed ischemic postconditioning.[22] Similar results were obtained 24 h after the onset of reperfusion (**Figures 6C** and **6E**). We thus found a linear correlation between infarct size and time delay for TD injection after the onset of reperfusion whether measured after 1 h-reperfusion (r^2= 0.92; **Figure 6B**) or 24 h-reperfusion (r^2= 0.83; **Figure 6C**). There was no statistical difference between AR/LV among groups after 1 h or 24 h-reperfusion (**Table S2** and **Figure S6**).

4. Discussion

Our study demonstrates the potent cardioprotective effects of the anti-apoptotic peptide Tat-DAXXp (TD) targeting the FAS-dependent pathway during ischemia-reperfusion injury. *In vitro*, this peptide was efficiently internalized in primary cardiomyocytes and provided anti-apoptotic effects after an apoptotic stress. *In vivo*, a single bolus of TD injected intravenously 5 min before reperfusion in a murine myocardial IR model decreased infarct size by 48% after 24 h reperfusion without any side effects probably in relation with its rapid degradation and elimination. Furthermore, cardioprotection was still efficient after delayed administration up to 30 min after reperfusion. Mechanistically, cardioprotection was

supported by both anti-apoptotic and pro-survival effects, and an improvement of the myocardial functional recovery was evidenced in *ex vivo* experiments. Importantly, TD treatment reduced mouse early post-infarction mortality by 67%. Altogether, these results suggest that TD treatment leads to a potent cardioprotection.

Prosurvival and apoptotic pathways are intricated and finely regulated with redundant mechanisms to strongly control cell fate after IR stress (**Figure 7A**).[18, 23] The death receptor/extrinsic and mitochondrial/intrinsic apoptotic pathways are the most heavily studied pathways of regulated cell death in myocardial IR injury. Once activated, these two apoptotic pathways initiate a cascade of caspases converging on mitochondria and leading to cell destruction. The involvement of the FAS receptor was reported to play a key role in myocardial IR-induced cell apoptosis in keeping with high levels of circulating FAS Ligand in the blood of AMI patients.[24-26] However, initiation of the FAS-dependent apoptotic cascade is induced by the binding of at least one of the two adaptor proteins, FADD and DAXX, to the intracellular region of the FAS receptor. FADD (*Fas-Associated protein with Death Domain*) then transduces death signals by activating caspase 8 within the DISC (*Death-Inducing Signal Complex*). Independently of FADD, phosphorylated DAXX relocalizes upon oxidative stress from the nucleus to the cytoplasm, interacts with FAS and activates the JNK pathway leading to cell death.[13] DAXX is able to activate the intrinsic pathway *via* the JNK-BAX-dependent crosstalk.[27, 28]

Our study shows that the interfering TD peptide provides a major cardioprotective effect when injected at the onset of reperfusion (**Figure 7B**). The resulting anti-apoptotic effect was evidenced first by a drastic decrease in specific DNA fragmentation in the myocardium after IR, corroborating our previous studies on cardioprotection.[5, 22, 29] As expected, because FAS:DAXX interaction was prevented, the downstream activation of the JNK/caspase 3 pathway was down-regulated upon TD treatment. The expression of BAD protein (a *Bcl-2-*

Associated Death promoter facilitating BAX/BAK activation) and the level of activated caspase 9, both mediators of the intrinsic pathway, were down-regulated, probably due to the mitochondrial crosstalk downstream JNK activation.[27] Consistently, co-administration of cyclosporin A (inhibitor of the mitochondrial permeability transition pore opening by interacting with cyclophilin D) and TD in our murine IR model did not provide any additive cardioprotection (data not shown). Interestingly, we evidenced that TD treatment was able to also decrease the FADD-caspase 8 extrinsic pathway probably due to its impact on DAXX-FADD cooperativity within the DISC as already observed in T-cells overexpressing DAXX-DN.[30] However and of great interest, TD peptide treatment was not associated in our study with a deleterious reduction of DAXX protein level, which could result in unexpected pro-apoptotic effects as reported in the case of siRNA DAXX silencing.[10] Altogether, these data show that TD treatment was able to decrease apoptosis upstream in the apoptotic signaling cascade by acting on both the extrinsic and intrinsic cascades. Finally, activation of effector caspase 3 was decreased resulting in a drastic decrease in DNA fragmentation and in HSP70 protein level, a hallmark of proteotoxic stress[19] leading to a potent cardioprotection. Studies in the literature have reported that HSP70 protein expression is strongly up-regulated during FAS-induced apoptosis *in vitro* and during myocardial IR in order to protect the cells against IR injury *via* a suppression of reactive oxygen species generation and by inhibiting cell apoptosis.[19, 31-33] Upon TD treatment, HSP70 protein level was reduced as compared to non-treated IR hearts suggesting that TD plays a key role in early cardioprotection.These results are of great interest because high levels of HSP70 are detected in the serum of patients with heart failure.[34]

Interestingly, cardioprotection afforded by TD treament was also related to an activation of survival pathways.[35, 36] We investigated the expression of proteins involved in the RISK (*Reperfusion Injury Salvage Kinase*) pathway including ERK1/2 and PI3kinase-AKT, which

both play crucial roles in preventing reperfusion injury in the myocardium. In both cases, our results show an activation of these survival kinases after TD treatment. ERK1/2 activation is associated with a protection against apoptosis in cardiac myocytes and to a reduction of IR injury in the heart *in vivo*.[35, 36] These results are also consistent with those already obtained in DAXX-DN mice that are cardioprotected against reperfusion injury.[29]

As already mentioned, DAXX is described as a dual protein with both anti-apoptotic and pro-apoptotic roles depending on its subcellular localization, nucleus *versus* cytoplasm, respectively[21, 27, 37-39]. Such a dual role requires a fine tuning of its nucleo-cytoplasmic ratio by phosphorylation, nuclear export, positive ASK1-SEK1-JNK[38] and negative ASK1-JIP (*JNK Interacting Protein*)[40] feedback loops in order to control the balance between survival and death, making complex mechanistic studies (See Supplementary Results 2.6). Our study performed in hearts subjected to IR *ex vivo* shows that, upon TD treatment, DAXX phosphorylation was 37%-decreased compared to IR condition. This is in accordance with the observed higher nuclear localization of DAXX after TD treatment compared to IR. These results were further confirmed by evaluating pDAXX levels 15 min after the onset of reperfusion. Our data show that, at this time point, pDAXX levels represents 63% of that measured in the 1 h-IR group (**Figure S9**) despite an obvious delayed cardioprotection characterized by a 42% decrease in both infarct size and soluble nucleosome ($TD_{\Delta 15}$ *versus* Tat; see **Figures 6B,D**). This suggests that DAXX export from the nucleus to the cytoplasm after phosphorylation occurs within the first minutes of the wavefront of IR injury[22] even in the presence of the peptide. Blocking DAXX trafficking was identified as a potential therapeutic target for ischemic injury in hippocampal neurons.[20, 41] Our data suggest that DAXX nuclear trafficking may be indirectly influenced by TD treatment as a result of its impact on both apoptotic and survival pathways as well as on the feedback loops controlling DAXX nucleo-cytoplasmic ratio (see **Figure 7**).

In conclusion, TD peptide treatment appears as a particularly relevant therapeutic strategy in view of the key and specific role played by DAXX in the upstream events of reperfusion-induced apoptotic pathways. Targeting FAS:DAXX interaction from the extrinsic pathway also indirectly reduced the activation of the intrinsic (JNK-BAX crosstalk) cascade thus allowing a complete inhibition of reperfusion injury with a single pharmacological agent. Indeed, a single bolus administration of the TD anti-apoptotic peptide at low dose was sufficient to trigger an effective cardioprotection mainly *via* a reduction of apoptosis during the requested time window. Our data indeed indicate that TD decreases both apoptosis and infarct size when administered up to 30 min after the re-opening of the occluded coronary artery. This perspective of delayed application, which is exactly in agreement with the delayed post-conditioning previously reported,[22] is clinically important since it offers the possibility to treat a larger number of patients including those already reperfused with thrombolytic agents before hospital admission. However, for further clinical translation, a detailed evaluation of the mechanism by which TD interacts with the FAS:DAXX protein complex as well as a determination of TD long-term cardioprotection in an IR murine model as well as in clinical relevant animal models will be important to fully understand the molecular effect of the peptide during reperfusion.

6. Funding

This work was supported by the Agence Nationale pour la Recherche (ANR-08-Genopat-031, SBL, BL, PB - ANR-12-EMMA-0009, SBL, PB), by FRM (PB), by the "Fonds Européen de Développement Régional" (FEDER grant #43457, SBL) and Région Languedoc-Roussillon and by a CNRS-SERVIER collaboration contract (#098976) with the participation of the SATT AxLR (contract #099482) and Eurobiodev (contract #099483).

7. Acknowledgements

The authors wish to thank the Biocampus mouse facility and Dominique Haddou for animal care. We acknowledge the MRI imaging facility, member of the national infrastructure France-BioImaging supported by the French National Research Agency (ANR-10-INBS-04, «Investments for the future»). The authors thank Christelle Redt, Carlota Fernández Rico, Bastien Lautrec (IGF) and Jean-Michel Giorgi (DIMNP) for their technical assistance as well as the group of Dr. Rudolf Volkmer (Institut für Medizinische Immunologie, Berlin) for peptide synthesis. Additionally, the authors are very grateful to Alexander Prieur and Maud Facellière (Eurobiodev) for technical assistance and fruitfull discussions.

8. Conflict of Interest: none declared.

9. References

1. Braunwald E. Myocardial reperfusion, limitation of infarct size, reduction of left ventricular dysfunction, and improved survival. Should the paradigm be expanded? Circulation 1989;79:441-444.

2. McGovern PG, Pankow JS, Shahar E, Doliszny KM, Folsom AR, Blackburn H, Luepker RV. Recent trends in acute coronary heart disease--mortality, morbidity, medical care, and risk factors. The Minnesota Heart Survey Investigators. N Engl J Med 1996;334:884-890.

3. Zhao ZQ, Nakamura M, Wang NP, Wilcox JN, Shearer S, Ronson RS, Guyton RA, Vinten-Johansen J. Reperfusion induces myocardial apoptotic cell death. Cardiovasc Res 2000;45:651-660.

4. Zhao ZQ, Velez DA, Wang NP, Hewan-Lowe KO, Nakamura M, Guyton RA, Vinten-Johansen J. Progressively developed myocardial apoptotic cell death during late phase of reperfusion. Apoptosis 2001;6:279-290.

5. Boisguerin P, Redt-Clouet C, Franck-Miclo A, Licheheb S, Nargeot J, Barrere-Lemaire S, Lebleu B. Systemic delivery of BH4 anti-apoptotic peptide using CPPs prevents cardiac ischemia-reperfusion injuries in vivo. J Control Release 2011;156:146-153.

6. Piot CA, Martini JF, Bui SK, Wolfe CL. Ischemic preconditioning attenuates ischemia/reperfusion-induced activation of caspases and subsequent cleavage of poly(ADP-ribose) polymerase in rat hearts in vivo. Cardiovasc Res 1999;44:536-542.

7. Yaoita H, Ogawa K, Maehara K, Maruyama Y. Attenuation of ischemia/reperfusion injury in rats by a caspase inhibitor. Circulation 1998;97:276-281.

8. Cung TT, Morel O, Cayla G, Rioufol G, Garcia-Dorado D, Angoulvant D, Bonnefoy-Cudraz E, Guerin P, Elbaz M, Delarche N, Coste P, Vanzetto G, Metge M, Aupetit JF, Jouve B, Motreff P, Tron C, Labeque JN, Steg PG, Cottin Y, Range G, Clerc J, Claeys MJ, Coussement P, Prunier F, Moulin F, Roth O, Belle L, Dubois P, Barragan P, Gilard M, Piot C, Colin P, De Poli F, Morice MC, Ider O, Dubois-Rande JL, Unterseeh T, Le Breton H, Beard T, Blanchard D, Grollier G, Malquarti V, Staat P, Sudre A, Elmer E, Hansson MJ, Bergerot C, Boussaha I, Jossan C, Derumeaux G, Mewton N, Ovize M. Cyclosporine before PCI in Patients with Acute Myocardial Infarction. N Engl J Med 2015;373:1021-1031.

9. Lefer DJ, Marban E. Is Cardioprotection Dead? Circulation 2017;136:98-109.

10. Chen LY, Chen JD. Daxx silencing sensitizes cells to multiple apoptotic pathways. Mol Cell Biol 2003;23:7108-7121.

11. Ko YG, Kang YS, Park H, Seol W, Kim J, Kim T, Park HS, Choi EJ, Kim S. Apoptosis signal-regulating kinase 1 controls the proapoptotic function of death-associated protein (Daxx) in the cytoplasm. J Biol Chem 2001;276:39103-39106.

12. Song JJ, Lee YJ. Catalase, but not MnSOD, inhibits glucose deprivation-activated ASK1-MEK-MAPK signal transduction pathway and prevents relocalization of Daxx:

hydrogen peroxide as a major second messenger of metabolic oxidative stress. J Cell Biochem 2003;90:304-314.

13. Chang HY, Nishitoh H, Yang X, Ichijo H, Baltimore D. Activation of apoptosis signal-regulating kinase 1 (ASK1) by the adapter protein Daxx. Science 1998;281:1860-1863.

14. Vives E, Brodin P, Lebleu B. A truncated HIV-1 Tat protein basic domain rapidly translocates through the plasma membrane and accumulates in the cell nucleus. J Biol Chem 1997;272:16010-16017.

15. Arakawa M, Yasutake M, Miyamoto M, Takano T, Asoh S, Ohta S. Transduction of anti-cell death protein FNK protects isolated rat hearts from myocardial infarction induced by ischemia/reperfusion. Life Sci 2007;80:2076-2084.

16. Miyaji Y, Walter S, Chen L, Kurihara A, Ishizuka T, Saito M, Kawai K, Okazaki O. Distribution of KAI-9803, a novel delta-protein kinase C inhibitor, after intravenous administration to rats. Drug Metab Dispos 2011;39:1946-1953.

17. Souktani R, Pons S, Guegan C, Bouhidel O, Bruneval P, Zini R, Mandet C, Onteniente B, Berdeaux A, Ghaleh B. Cardioprotection against myocardial infarction with PTD-BIR3/RING, a XIAP mimicking protein. J Mol Cell Cardiol 2009;46:713-718.

18. Wu MY, Yiang GT, Liao WT, Tsai AP, Cheng YL, Cheng PW, Li CY, Li CJ. Current Mechanistic Concepts in Ischemia and Reperfusion Injury. Cell Physiol Biochem 2018;46:1650-1667.

19. Chen Z, Shen X, Shen F, Zhong W, Wu H, Liu S, Lai J. TAK1 activates AMPK-dependent cell death pathway in hydrogen peroxide-treated cardiomyocytes, inhibited by heat shock protein-70. Mol Cell Biochem 2013;377:35-44.

20. Niu YL, Li C, Zhang GY. Blocking Daxx trafficking attenuates neuronal cell death following ischemia/reperfusion in rat hippocampus CA1 region. Arch Biochem Biophys 2011;515:89-98.

21. Song JJ, Lee YJ. Role of the ASK1-SEK1-JNK1-HIPK1 signal in Daxx trafficking and ASK1 oligomerization. J Biol Chem 2003;278:47245-47252.

22. Roubille F, Franck-Miclo A, Covinhes A, Lafont C, Cransac F, Combes S, Vincent A, Fontanaud P, Sportouch-Dukhan C, Redt-Clouet C, Nargeot J, Piot C, Barrere-Lemaire S. Delayed postconditioning in the mouse heart in vivo. Circulation 2011;124:1330-1336.

23. Beere HM. Death versus survival: functional interaction between the apoptotic and stress-inducible heat shock protein pathways. J Clin Invest 2005;115:2633-2639.

24. Jeremias I, Kupatt C, Martin-Villalba A, Habazettl H, Schenkel J, Boekstegers P, Debatin KM. Involvement of CD95/Apo1/Fas in cell death after myocardial ischemia. Circulation 2000;102:915-920.

25. Lee P, Sata M, Lefer DJ, Factor SM, Walsh K, Kitsis RN. Fas pathway is a critical mediator of cardiac myocyte death and MI during ischemia-reperfusion in vivo. Am J Physiol Heart Circ Physiol 2003;284:H456-463.

26. Shimizu M, Fukuo K, Nagata S, Suhara T, Okuro M, Fujii K, Higashino Y, Mogi M, Hatanaka Y, Ogihara T. Increased plasma levels of the soluble form of Fas ligand in patients with acute myocardial infarction and unstable angina pectoris. J Am Coll Cardiol 2002;39:585-590.

27. Song JJ, Lee YJ. Daxx deletion mutant (amino acids 501-625)-induced apoptosis occurs through the JNK/p38-Bax-dependent mitochondrial pathway. J Cell Biochem 2004;92:1257-1270.

28. Luo X, Budihardjo I, Zou H, Slaughter C, Wang X. Bid, a Bcl2 interacting protein, mediates cytochrome c release from mitochondria in response to activation of cell surface death receptors. Cell 1998;94:481-490.

29. Roubille F, Combes S, Leal-Sanchez J, Barrere C, Cransac F, Sportouch-Dukhan C, Gahide G, Serre I, Kupfer E, Richard S, Hueber AO, Nargeot J, Piot C, Barrere-Lemaire S.

Myocardial expression of a dominant-negative form of Daxx decreases infarct size and attenuates apoptosis in an in vivo mouse model of ischemia/reperfusion injury. Circulation 2007;116:2709-2717.

30. Leal-Sanchez J, Couzinet A, Rossin A, Abdel-Sater F, Chakrabandhu K, Luci C, Anjuere F, Stebe E, Hancock D, Hueber AO. Requirement for Daxx in mature T-cell proliferation and activation. Cell Death Differ 2007;14:795-806.

31. Choudhury S, Bae S, Ke Q, Lee JY, Kim J, Kang PM. Mitochondria to nucleus translocation of AIF in mice lacking Hsp70 during ischemia/reperfusion. Basic Res Cardiol 2011;106:397-407.

32. Gerner C, Frohwein U, Gotzmann J, Bayer E, Gelbmann D, Bursch W, Schulte-Hermann R. The Fas-induced apoptosis analyzed by high throughput proteome analysis. J Biol Chem 2000;275:39018-39026.

33. Zhao Y, Wang W, Qian L. Hsp70 may protect cardiomyocytes from stress-induced injury by inhibiting Fas-mediated apoptosis. Cell Stress Chaperones 2007;12:83-95.

34. Genth-Zotz S, Bolger AP, Kalra PR, von Haehling S, Doehner W, Coats AJ, Volk HD, Anker SD. Heat shock protein 70 in patients with chronic heart failure: relation to disease severity and survival. Int J Cardiol 2004;96:397-401.

35. Hausenloy DJ, Yellon DM. Reperfusion injury salvage kinase signalling: taking a RISK for cardioprotection. Heart Fail Rev 2007;12:217-234.

36. Hausenloy DJ, Yellon DM. Ischaemic conditioning and reperfusion injury. Nat Rev Cardiol 2016;13:193-209.

37. Khelifi AF, D'Alcontres MS, Salomoni P. Daxx is required for stress-induced cell death and JNK activation. Cell Death Differ 2005;12:724-733.

38. Song JJ, Lee YJ. Tryptophan 621 and serine 667 residues of Daxx regulate its nuclear export during glucose deprivation. J Biol Chem 2004;279:30573-30578.

39. Yang X, Khosravi-Far R, Chang HY, Baltimore D. Daxx, a novel Fas-binding protein that activates JNK and apoptosis. Cell 1997;89:1067-1076.

40. Song JJ, Lee YJ. Dissociation of Akt1 from its negative regulator JIP1 is mediated through the ASK1-MEK-JNK signal transduction pathway during metabolic oxidative stress: a negative feedback loop. J Cell Biol 2005;170:61-72.

41. Yang R, Hu K, Chen J, Zhu S, Li L, Lu H, Li P, Dong R. Necrostatin-1 protects hippocampal neurons against ischemia/reperfusion injury via the RIP3/DAXX signaling pathway in rats. Neurosci Lett 2017;651:207-215.

10. Figure legends

Figure 1: Internalization and anti-apoptotic properties of Tat-DAXXp in cardiomyocytes.

(**A**) Cellular internalization was assessed by flow cytometry in cardiomyocytes incubated with carboxyfluorescein (CF)-labeled TD or CF-DAXXp (1 µmol/L) for 1 h. Untreated cells represent the negative control (Ctrl). Data plotted as scatter dot blots and mean ± SD with n=3 independent cultures. (**B**) Representative image of cultured cardiomyocytes incubated with 1 µmol/L CF-TD incubated for 1 h or 4 h. Cell nuclei were stained with Hoechst-dye (blue). Bar scale = 10 µm; (**C, D**) Specific DNA fragmentation was measured in cardiomyocytes treated with staurosporin (STS) for 6 h with or without peptides (concentrations in µmol/L noted in parentheses) and allowed to recover during 40 h. Data (plotted as scatter dot blots and mean ± SD with n=5 independent cultures) were compared using Kruskal-Wallis (Dunn's *post hoc* test) and were noted * for $p<0.05$ *versus* Tat and # for $p<0.05$ *versus* TDS.

Figure 2: Improved functional recovery upon Tat-DAXXp treatment *ex vivo.*

(A) Mouse hearts were perfused on a Langendorff system and subjected to 30 min of global **(B,C)** or 40 min of regional **(D)** ischemia followed by 1 h-reperfusion. 1 µmol/L TD or TDS were perfused during the first minute of reperfusion; **(B)** Scatter dot blots and mean ± SD were plotted for infarct size (% LV). A drastic decrease in infarct size was observed after TD treatment *versus* TDS (21.34 ± 3.48 for TD, n=6 *versus* 38.51 ± 7.62 for TDS, n=9; p*=0.012) which did not provide any cardioprotection *versus* IR (38.51 ± 7.62 for TDS, n=9 *versus* 40.68 ± 2.85 for IR, n=6, ns for p>0.999). Statistical analysis was performed using Kruskal-Whallis with the Dunn's post test for multiple comparison. Representative pictures of tissue samples after phtalocyanin blue and TTC-dye dual coloration for IR, TD and TDS administered at 1 mg/kg. Scale bar: 2 mm. (**C**) Developed tension evaluated with the DMT myograph during ischemia (grey rectangle) and reperfusion (TD, n=6 *versus* TDS, n=5; p***=0.0009). For repeated measures, data (plotted as mean ± SD) were compared using two-way RM ANOVA and the Tukey's post-test. (**D**) Coronary flow measured on the EMKA system in hearts treated by TD (n=6) *versus* IR (IR; n=6); p**=0.0072. For repeated measures, data (plotted as mean ± SD) were compared using two-way RM ANOVA and the Sidak's post-test.

Figure 3: Effect of TD in mice subjected to an IR protocol *in vivo*.

(**A**) Whole-body SPECT/CT *in vivo* imaging of ^{125}I-TD in IR (40 minutes ischemia - 3 h reperfusion) *versus* non operated Ctrl mice at 3 h post-injection. From left to right, representative images with coronal, sagittal, and transverse views of tracer activity. Please note ^{125}I-TD localization in the heart (white arrow) with a more pronounced signal in the ischemic condition (IR mouse) *versus* control (Ctrl). L for left side and R for right. Scale bar: 5 mm. (**B**) Quantification of *in vivo* images of ^{125}I-TD whole-body distribution at indicated

time points (0 h, 3 h, 6 h and 24 h) post-injection in control (Ctrl; n=3) and IR mice treated (n=2).

(**C,D**) Scatter dot blots and mean ± SD for infarct size (% of area at risk) was measured after 1 h (**C**) or 24 h (**D**) of reperfusion in mice subjected to 40 min-ischemia and treated with Tat, TDS or TD intravenously 5 min before reperfusion at the indicated doses (in mg/kg). Representative pictures of tissue samples after phtalocyanin blue and TTC-dye dual coloration for Tat, TD and TDS administered at 1 mg/kg. A drastic decrease in infarct size at 1 h of reperfusion was observed after TD treatment *versus* Tat (15.54 ± 6.91 for TD, n=11 *versus* 38.37 ± 8.46 for Tat, n=14; p****<0.0001). Note that n= 6 for TD (0.1 mg/kg) and TD (10 mg/kg). (**D**) Same results at 24 h-reperfusion: 17.19 ± 5.16 for TD, n=8 *versus* 33.29 ± 6.07 for Tat, n=17; p**=0.001. Note that n= 7 for TD (0.1 mg/kg) and n=6 for TD (10 mg/kg). Data were compared using Kruskal-Whallis with the Dunn's post test. Bar scale: 2 mm.

Figure 4: Anti-apoptotic effect of Tat-DAXXp treatment

Internucleosomal DNA fragmentation was determined by ELISA in IR mice treated with Tat, TDS and TD (at indicated doses in mg/kg) after 1 h (**A**) or 24 h (**B**) of reperfusion. Scatter dot blots and mean ± SD show the I/NI ratio corresponding to the ratio of soluble nucleosomes in the ischemic *versus* the non-ischemic portion of LV tissues. A drastic decrease in soluble nucleosome ratio at 1 h of reperfusion was observed after TD treatment *versus* Tat (1.61 ± 0.44 for TD, n=6 *versus* 4.09 ± 0.75 for Tat, n=11; p****<0.0001). Note that n=7 for TDS, n=10 for TD (0.1 mg/kg) and n=6 for TD (10 mg/kg). Same results at 24 h-reperfusion: 1.57 ± 0.37 for TD, n=6 *versus* 4.01 ± 1.33 for Tat, n=13; p****<0.0001. Note that n=10 for TDS, n=6 for TD (0.1 mg/kg) and n=6 for TD (10 mg/kg). Data were compared using Kruskal-Whallis with the Dunn's post test.

(**C-E**): *Western blot* analysis was performed from LV protein extracts from non-treated or TD (1 μM/L) murine IR hearts (*ex vivo*). Scatter dot blots and mean ± SD were plotted for (**C**) DAXX (p=0.1775; n=6 for each group), pJNK/JNK ratio (p**=0.0022; n=6 for each group) and pro-caspase 3 (p*=0.0173; n=6 for each group); (**D**): FADD (p*=0.0260; n=6 for each group), FAS (p=0.3939; n=6 for each group) and cleaved caspase 8 (p**=0.0022; n=6 for each group); (**E)**, BAD (p**=0.0022; n=6 for each group), pro- (p*=0.0221; n=6 for IR and n=7 for TD) and cleaved caspase 9 (p**=0.0047; n=6 for IR and n=7 for TD). Representative gel blots are presented for each protein for the two conditions (IR *versus* TD). Tubulin, vinculin or α-actinin were used as protein loading control. Statistical analysis was performed using non-parametric Mann-Whitney test.

Figure 5: Mechanisms of TD cardioprotection

(**A-C**) *Western blot* analysis was performed from LV protein extracts from non-treated or TD (1 μmol/L; n=6) murine IR (n=6) hearts (*ex vivo*). Scatter dot blots and mean ± SD were plotted for (**A**), HSP70 (p*=0.0260) (**B**) and $pERK_{1/2}$ / $ERK_{1/2}$ (p*=0.0173) and (**C**) pAKT/AKT (p*=0.0130) ratios. Representative gel blots are presented for each protein for the two conditions (IR *versus* TD). Vinculin or α-actinin were used as protein loading control. Statistical analysis was performed using non-parametric Mann-Whitney test.

(**D**) Representatives images of cultured cardiomyoctes isolated from hearts subjected *ex vivo* to global IR without or with TD or Tat treatment compared to basal conditions. Bar scale=50 μm for DAXX, DAPI and merge images; bar scale=10 μm for enlargement inset.

(**E**) Percentages (mean ± SD) of cells expressing exclusively nuclear DAXX (ratio to DAXX positive cells) in cardiomyoctes isolated from hearts in basal conditions (n=3 independent cultures) or subjected *ex vivo* to global IR (n=5) in the presence or not of TD (33 ± 2 for TD, n=3 *versus* 9 ± 3 for Tat, n=3).

(**F)** Representative gel blots are presented for each protein for the two conditions obtained in *Western blot* analysis performed on LV protein extracts from Sham (n=6), IR (n=6), Tat (n=7) and TD (n=6) hearts. (**G**) Scatter dot blots and mean ± SD were plotted for pDAXX protein levels. Data were compared using non parametric Kruskal-Whallis test (Dunn's *post hoc* test) and statistical significance was noted for Sham p**= 0.0039 or ns for TD *versus* Tat.

Figure 6: Time window of cardioprotection.

(**A**) Mice were subjected to 40 min ischemia and reperfused for 1 h (**B, D**) or 24 h (**C, E**). TD (1 mg/kg) was injected 5 min before, or 15, 30 and 45 min (Δ15, Δ30 and Δ45, respectively) after the onset of reperfusion. At the end of the protocol, infarct size (in % of area at risk) and internucleosomal DNA fragmentation were quantified in LV. (**B, C**) Mean ± SD for infarct size/AR were plotted as a function of Δt (delay of TD injection, in min) and fitted as linear regressions (r^2= 0.92 in (**B**) and 0.83 in (**C**)). A dotted line for infarct size mean of Tat-treated animals was reported. A drastic decrease in infarct size at 1 h-reperfusion was observed when TD was injected 30 min post-reperfusion *versus* Tat treatment (25.12 ± 4.95 for $TD_{\Delta30}$, n=10 *versus* 38.37 ± 8.46 for Tat, n=14; p***=0.003). Please note that n=11 for TD, n=6 for $TD_{\Delta15}$ et n=9 for $TD_{\Delta45}$. Same results at 24 h-reperfusion: 23.62 ± 4.69 for $TD_{\Delta30}$, n=14 *versus* 33.29 ± 6.07 for Tat, n=17; p****<0.0001. Note that n=8 for TD, n=6 for $TD_{\Delta15}$ et n=9 for $TD_{\Delta45}$. Infarct size data (mean ± SD) were fitted by a linear regression model using the least squares method.

(**D, E**) Scatter dot blots and mean ± SD shown the DNA fragmentation for all groups described in (**A**). A drastic decrease in soluble nucleosome ratio at 1 h-reperfusion (**D**) was still observed when TD was injected up to 30 min post-reperfusion *versus* Tat treatment (2.58 ± 0.51 for $TD_{\Delta30}$, n=11 *versus* 4.09 ± 0.75 for Tat, n=11; p*=0.016). Note that n=6 for TD, n=6 for $TD_{\Delta15}$ and n=8 for $TD_{\Delta45}$. (**E**) Same results were observed at 24 h-reperfusion: 2.34 ±

0.71 for $TD_{\Delta 30}$, n=10 *versus* 4.01 ± 1.33 for Tat, n=13; p*=0.031. Please note that n=6 for TD, n=6 for $TD_{\Delta 15}$ and n=8 for $TD_{\Delta 45}$. Data (plotted as mean ± SD) were compared using non parametric Kruskal-Whallis test (Dunn's *post hoc* test). Statistical significance *versus* Tat noted with * and *versus* TD noted with #.

Figure 7: Schematic representation of apoptotic and survival cascades impacted by Tat-DAXXp treatment.

(**A**) Schema presenting the signaling apoptotic cascades activated during IR involving DAXX in the myocardium.

(**B**) Recapitulative schema presenting the impact of TD treatment administered at the onset of reperfusion and leading to the inhibition of both the extrinsic and intrinsic pathway as well as the activation of the survival kinases.

In both schemas the feeback loops regulating DAXX nucleo-cytoplasmic ratio are highlighted.

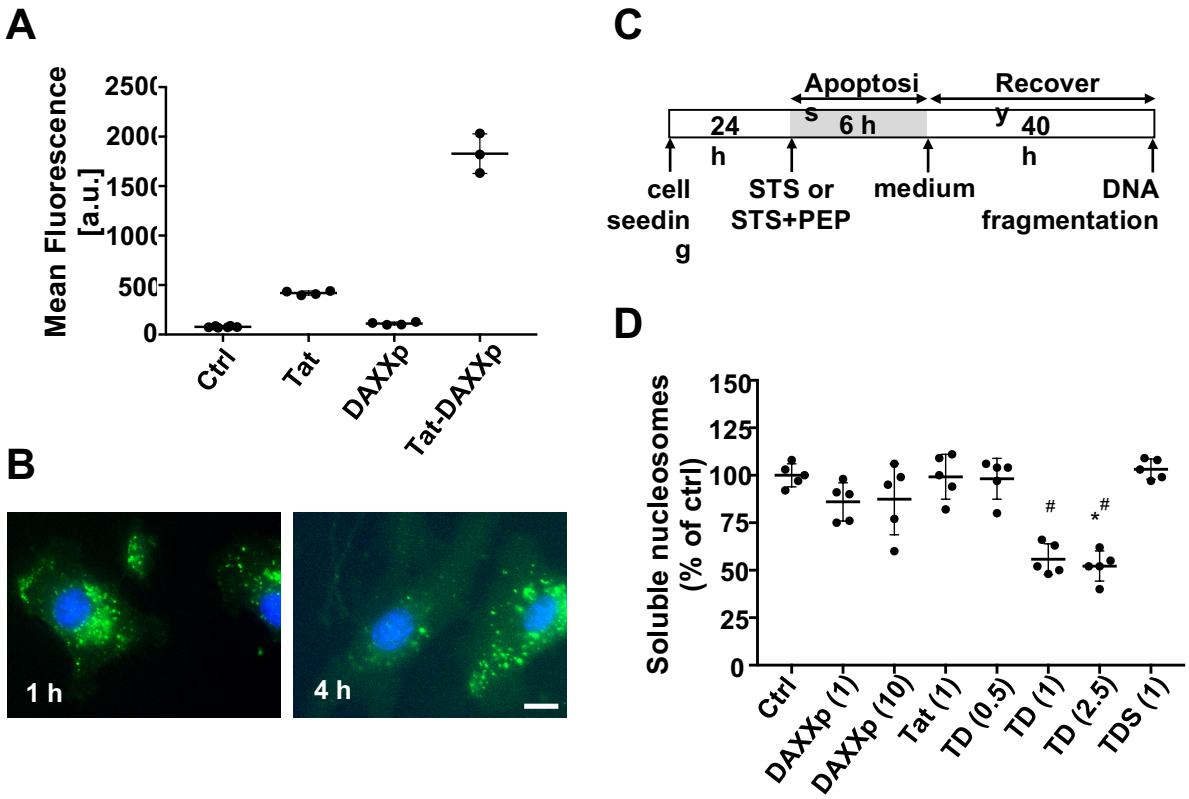
A
Mean Fluorescence [a.u.]
2500
2000
1500
1000
500
0
Ctrl
Tat
DAXXp
Tat-DAXXp
B
1 h
4 h
C
Apoptosis
Recovery
24 h
6 h
40 h
cell seeding
STS or STS+PEP
medium
DNA fragmentation
D
Soluble nucleosomes (% of ctrl)
150
125
100
75
50
25
0
Ctrl
DAXXp (1)
DAXXp (10)
Tat (1)
TD (0.5)
TD (1)
TD (2.5)
TDS (1)

Figure 1

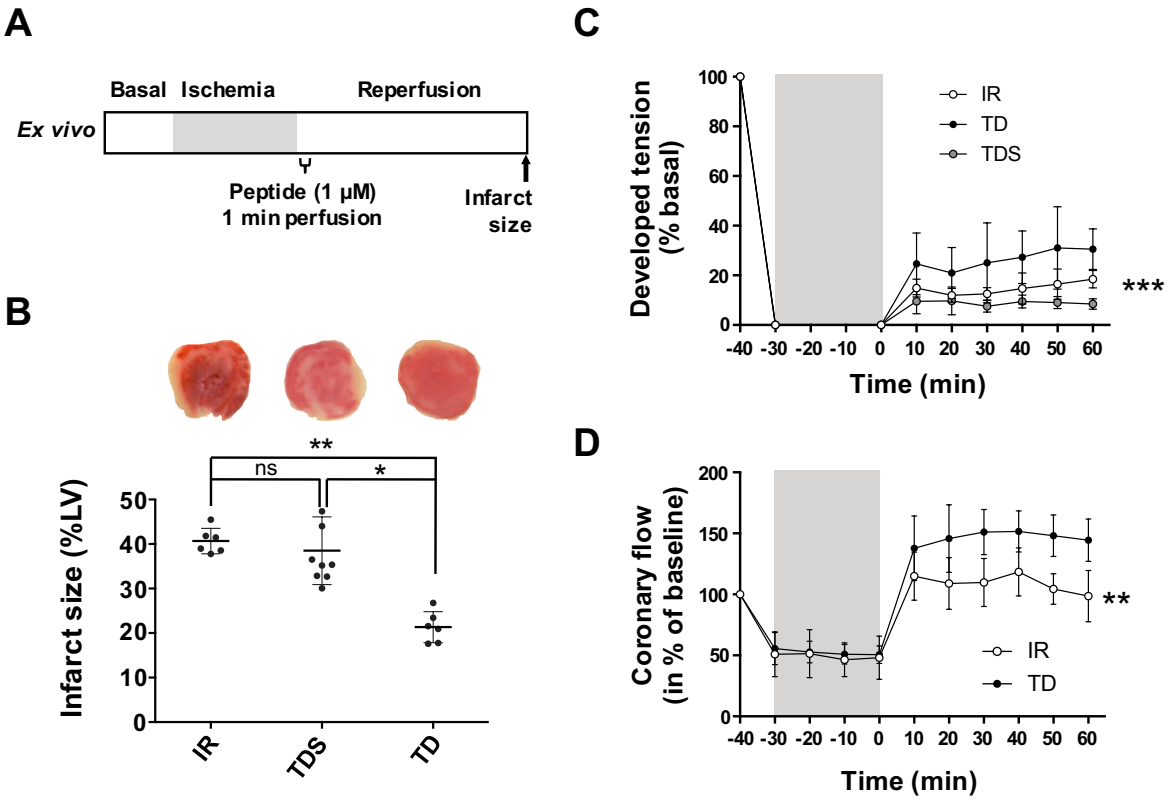
A
Basal
Ischemia
Reperfusion
Ex vivo
Peptide (1 µM)
1 min perfusion
Infarct size
B
Infarct size (%LV)
ns
**
*
IR
TDS
TD
C
Developed tension (% basal)
IR
TD
TDS
***
Time (min)
D
Coronary flow (in % of baseline)
IR
TD
**
Time (min)

Figure 2

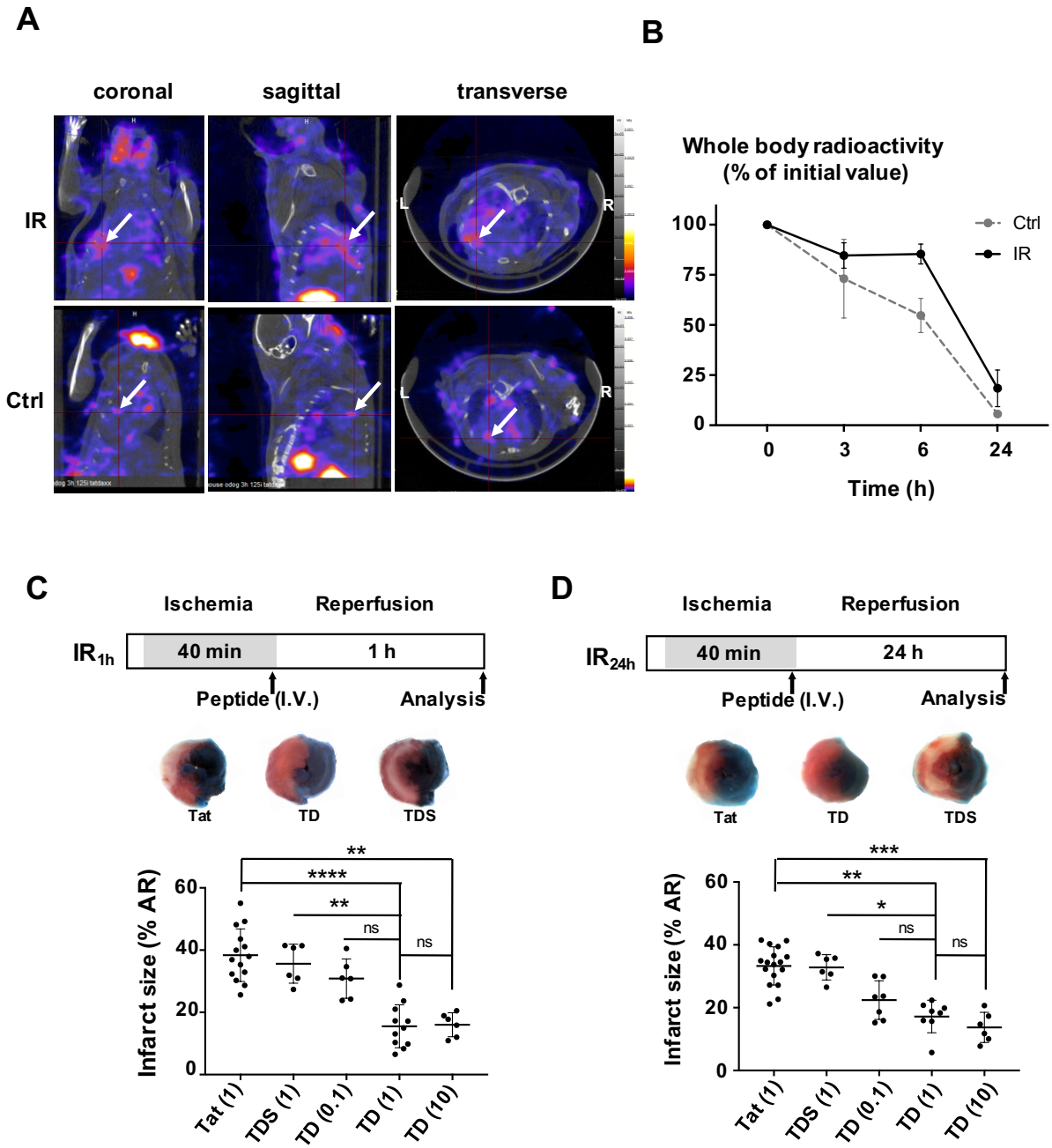
A
coronal
sagittal
transverse
IR
Ctrl
B
Whole body radioactivity
(% of initial value)
100
75
50
25
0
Ctrl
IR
0
3
6
24
Time (h)
C
Ischemia
Reperfusion
IR1h
40 min
1 h
Peptide (I.V.)
Analysis
Tat
TD
TDS
Infarct size (% AR)
60
40
20
0
**
****
**
ns
ns
Tat (1)
TDS (1)
TD (0.1)
TD (1)
TD (10)
D
Ischemia
Reperfusion
IR24h
40 min
24 h
Peptide (I.V.)
Analysis
Tat
TD
TDS
Infarct size (% AR)
60
40
20
0
***
**
*
ns
ns
Tat (1)
TDS (1)
TD (0.1)
TD (1)
TD (10)

Figure 3

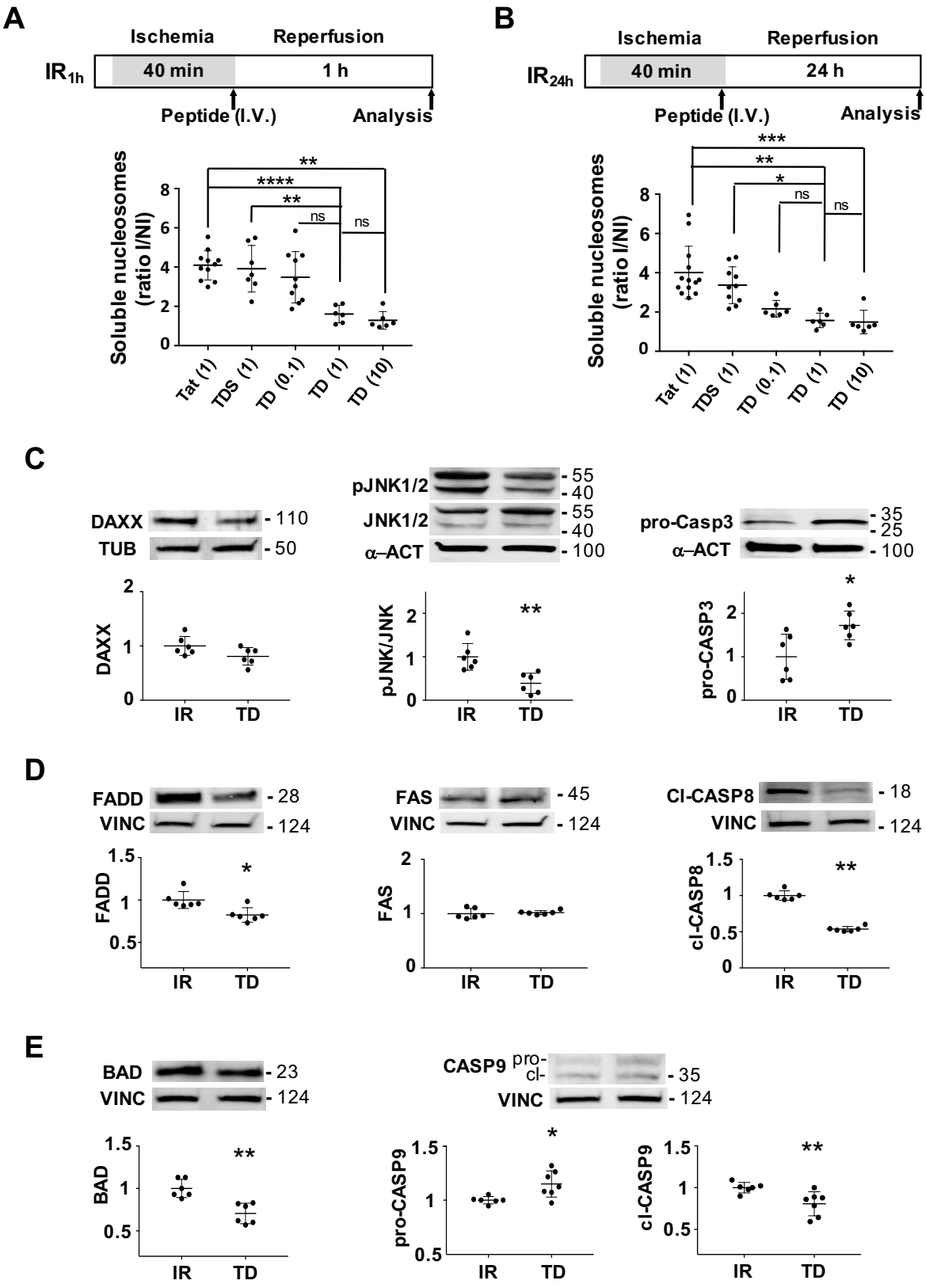
A
Ischemia
Reperfusion
IR1h
40 min
1 h
Peptide (I.V.)
Analysis
Soluble nucleosomes (ratio I/NI)
Tat (1)
TDS (1)
TD (0.1)
TD (1)
TD (10)
B
IR24h
24 h
C
DAXX
TUB
pJNK1/2
JNK1/2
α–ACT
pro-Casp3
pJNK/JNK
pro-CASP3
D
FADD
VINC
FAS
Cl-CASP8
cl-CASP8
E
BAD
CASP9 pro- cl-
pro-CASP9
cl-CASP9
IR
TD

Figure 4

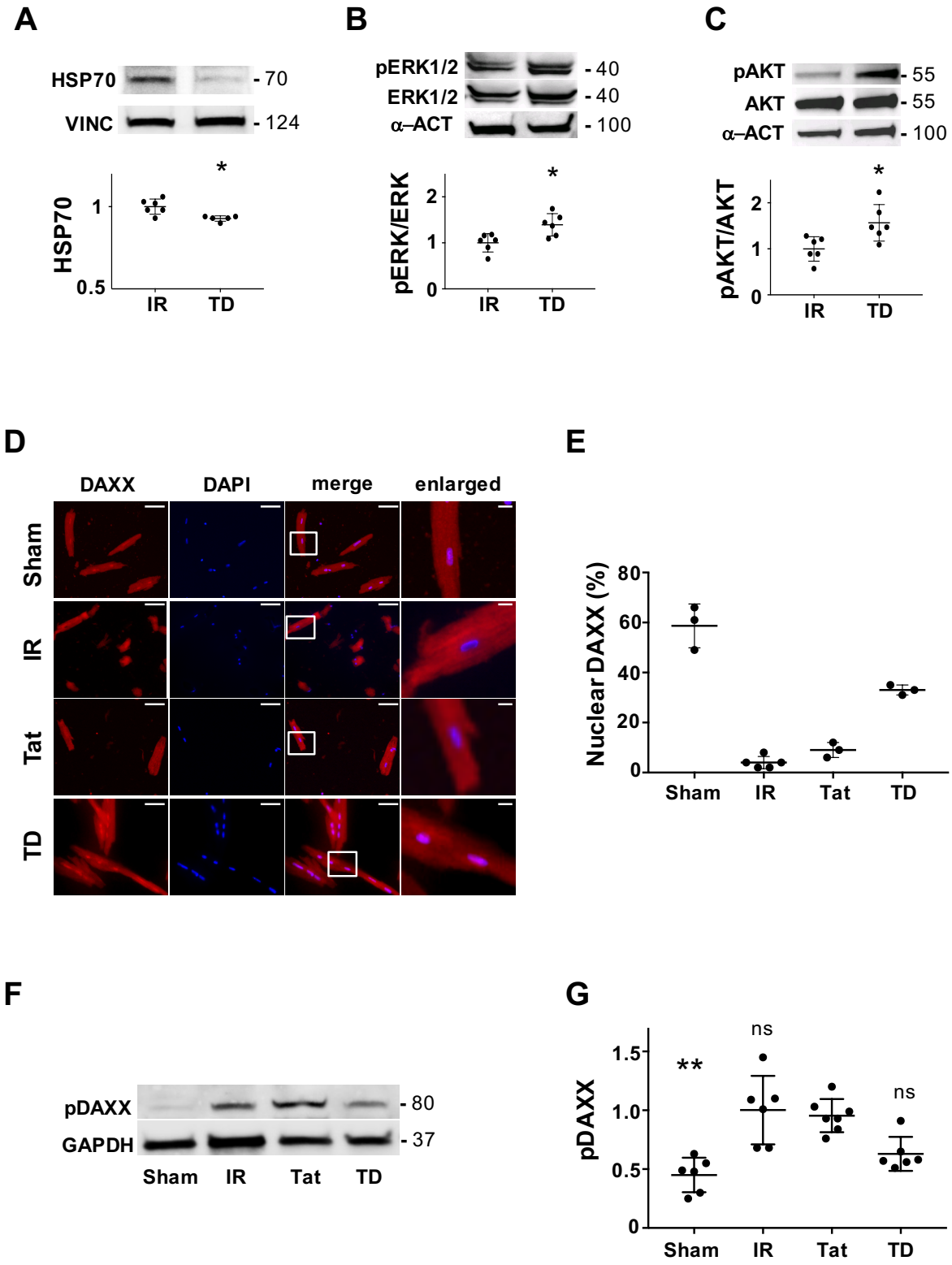
A
HSP70
VINC
70
124
HSP70
1
0.5
IR
TD
B
pERK1/2
ERK1/2
α–ACT
40
40
100
pERK/ERK
2
1
0
IR
TD
C
pAKT
AKT
α–ACT
55
55
100
pAKT/AKT
2
1
0
IR
TD
D
DAXX
DAPI
merge
enlarged
Sham
IR
Tat
TD
E
Nuclear DAXX (%)
80
60
40
20
0
Sham
IR
Tat
TD
F
pDAXX
GAPDH
80
37
Sham
IR
Tat
TD
G
pDAXX
1.5
1.0
0.5
0
**
ns
ns
Sham
IR
Tat
TD

Figure 5

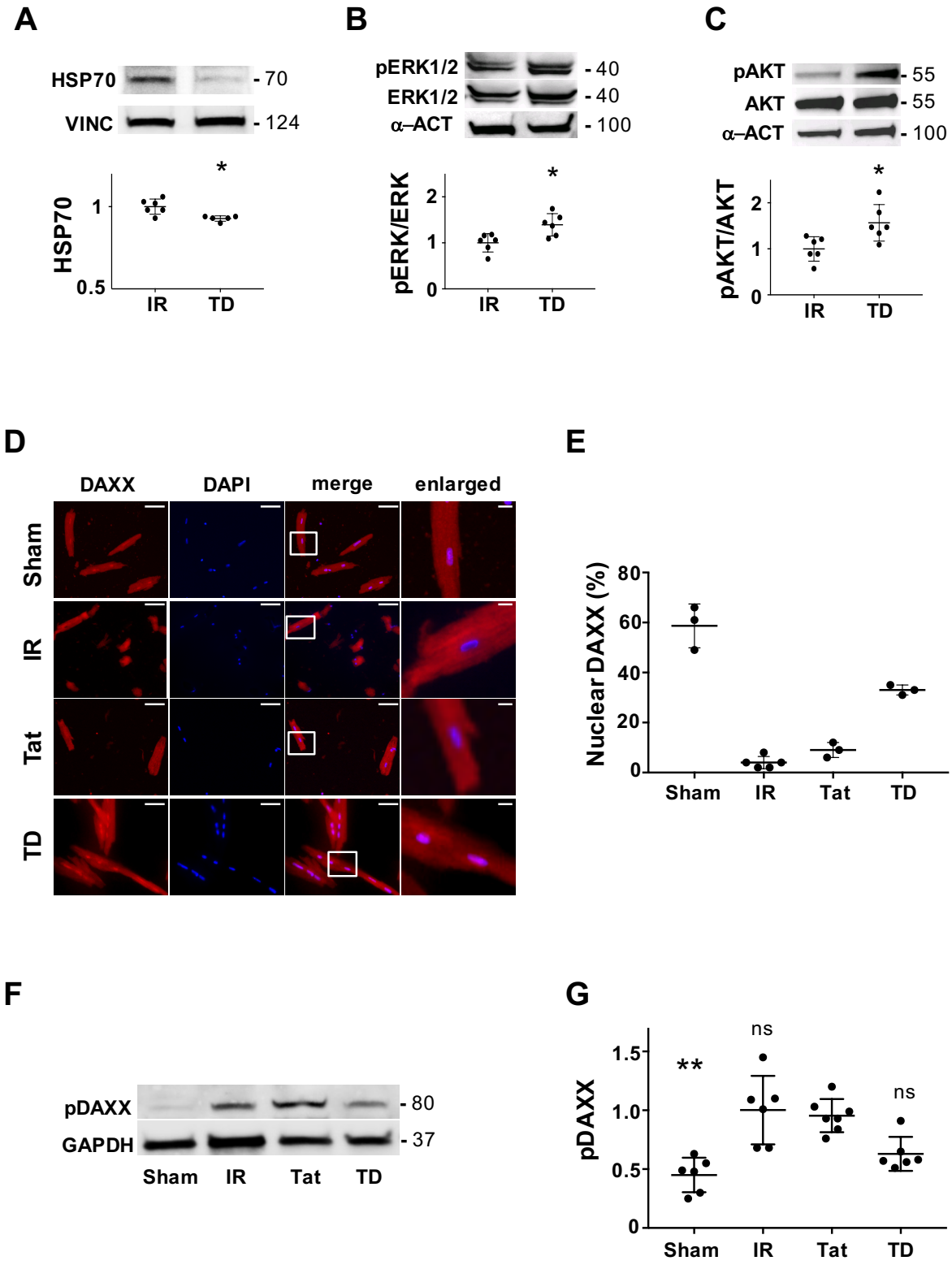
A
HSP70
VINC
70
124
HSP70
1
0.5
IR
TD
B
pERK1/2
ERK1/2
α–ACT
40
40
100
pERK/ERK
2
1
0
IR
TD
C
pAKT
AKT
α–ACT
55
55
100
pAKT/AKT
2
1
0
IR
TD
D
DAXX
DAPI
merge
enlarged
Sham
IR
Tat
TD
E
Nuclear DAXX (%)
80
60
40
20
0
Sham
IR
Tat
TD
F
pDAXX
GAPDH
80
37
Sham
IR
Tat
TD
G
pDAXX
1.5
1.0
0.5
0
**
ns
ns
Sham
IR
Tat
TD

Figure 6

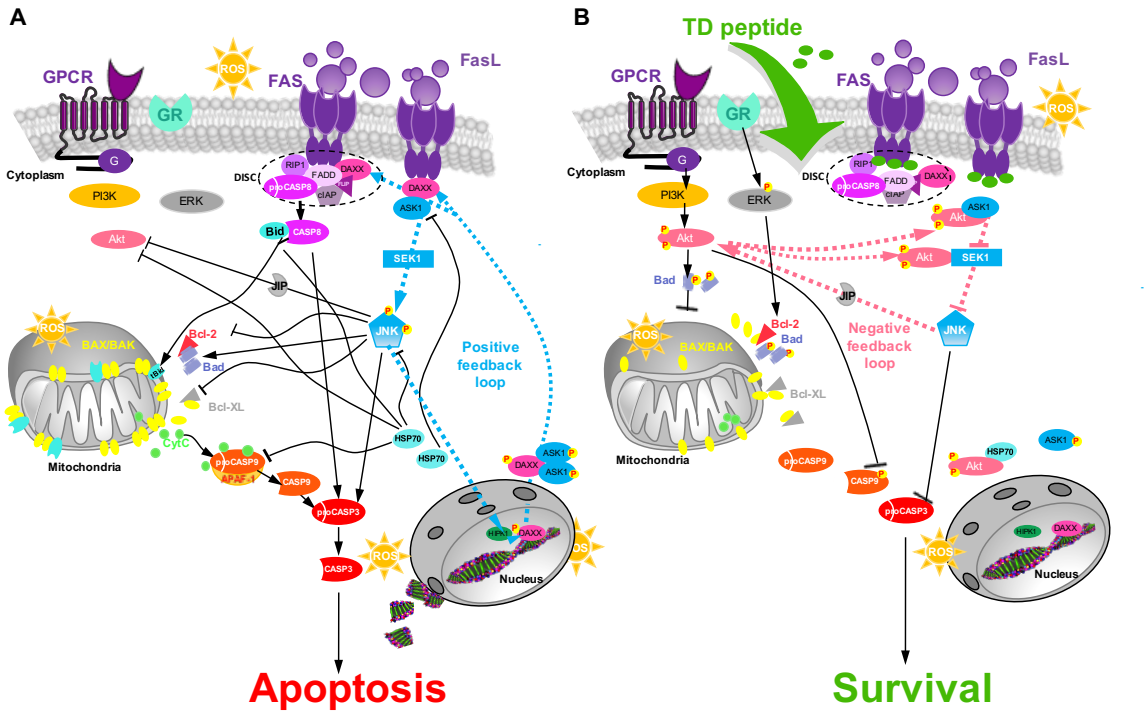
A
GPCR
GR
ROS
FAS
FasL
Cytoplasm
G
PI3K
ERK
DISC
RIP1
FADD
DAXX
proCASP8
cIAP
ASK1
Bid
CASP8
Akt
SEK1
JIP
JNK
ROS
BAX/BAK
Bcl-2
Bad
Bcl-XL
Positive feedback loop
Mitochondria
CytC
HSP70
proCASP9
APAF-1
CASP9
proCASP3
CASP3
ROS
HIPK1
DAXX
ASK1
Nucleus
Apoptosis
B
TD peptide
GPCR
GR
FAS
FasL
ROS
Cytoplasm
G
PI3K
ERK
DISC
RIP1
FADD
DAXX
proCASP8
cIAP
ASK1
Akt
SEK1
Bad
JIP
JNK
Negative feedback loop
ROS
BAX/BAK
Bcl-2
Bad
Bcl-XL
Mitochondria
proCASP9
CASP9
proCASP3
HSP70
ASK1
Akt
ROS
HIPK1
DAXX
Nucleus
Survival

Figure 7

A novel therapeutic peptide targeting myocardial reperfusion injury.

SUPPLEMENTARY MATERIAL

Boisguerin et al.

1. Supplemental methods

1.1. Peptide-array binding studies

Peptide libraries were generated by a MultiPep SPOTrobot (*INTAVIS Bioanalytical Instruments AG*) on N-modified CAPE-membranes[1] according to the standard SPOT synthesis.[2] The peptide array was prewashed with EtOH (1x10 min), washed with Tris-buffered saline (TBS, pH 8.0, 3x10 min), and blocked for 4 h with blocking buffer (blocking reagent; *Sigma-Genosys*) in TBS buffer (pH 8.0) containing 5% sucrose. Membranes were incubated with the polyhistidine-tagged intracellular region of the FAS receptor (10 µg/ml of iFasR; *Sigma-Aldrich*) in blocking buffer overnight at 4°C, and then washed with TBS (pH 8.0, 3x10 min). Bound intracellular FAS receptor was detected using a mouse anti-polyHis antibody (*Sigma-Aldrich*; 1:3,000 in blocking buffer, 2 h at room temperature) followed by horseradish-peroxidase conjugated anti-mouse antibody (*Calbiochem*; 1:2,000 in blocking buffer, 1 h at room temperature). Detection was carried out with Uptilight HRP blot chemiluminescent substrate (*Uptima*) with a 1 min exposure time. The signal intensities with background subtraction were recorded as biochemical light units (BLU) with a LumiImager (*Boehringer*) and analyzed using the LumiAnalyst software (*Boehringer*).

1.2. Peptide synthesis

Tat (13-mer), DAXXp (16-mer), Tat-DAXXp (TD; 29-mer), Tat-scrDAXXp (TDS; 29-mer corresponding to the scrambled version DAXXp coupled to Tat) as well as the other deriving sequences (see **Table S1**) were synthesized on resin by conventional Fmoc-chemistry [by the group of Dr. Volkmer (Charité, Berlin) or by Intavis AG].

For microscopy experiments, the peptides were labeled with 3,5-carboxyfluorescein (CF) as reported by Fischer *et al*.[3] or with Cy5.

All peptides were purified by quantitative RP-HPLC and characterized by analytical RP-HPLC and mass spectrometry to ensure a purity of >95%.

For SPECT-CT, TD sequence with an additional tyrosine residue (Y-TD) was labeled with ^{125}I (*Perkin-Elmer*; specific activity of 370 MBq/mg) using the IODO-GEN (*Pierce Chemical*) method and previously described protocols.[4]

1.3. Tat-DAXXp and DAXXp stability assays

The peptides were dissolved in 20% mouse serum (in house preparation) in water at 1 mg/mL concentration. The peptides were incubated at 37°C and at various times (0 h, 1 h, 2 h, 4 h, 8 h). 50 µmol/L of the solution was precipitated in 100 µmol/L 10% dichloroacetic acid (DCA) in H_2O/CH_3CN (50/50). For a better precipitation, the samples were kept overnight at -20°C. After a centrifugation (5 min, at 14,000 rpm), 50 µmol/L of the samples were injected for HPLC analysis (*Waters*). The peak areas (A [µV*sec]) of the different incubation times were determined and compared.

1.4. Cell cultures

<u>*Mouse myoblast cells*</u> (C2C12 – ATCC: CRL-1772™) were cultured in Dulbecco's Modified Eagle's Medium (DMEM, Gibco®, *Life Technologies*) supplemented with 10% (v/v) fetal bovine serum (FBS; *BioWest*), 1 mM Na pyruvate Gibco®, (*Life Technologies*), 1% (v/v) non-essential amino acids (100X, Gibco®; *Life Technologies*) and 1% (v/v) penicillin-streptomycin-neomycin (PSN, Gibco®; *Life Technologies*).

<u>*Primary neonate cardiomyocytes*</u> were isolated from 1- to 2-day-old C57BL/6J mice (*Charles River Laboratories*) ventricles by enzymatic digestion (type-4 collagenase; *Serlabo Technologies* and pancreatin, Gibco®**; *Life Technologies***) as described previously.[5] Freshly isolated cells were seeded in 90-mm Petri dishes to allow selective adhesion of cardiac

fibroblasts[6] in plating medium: 250 mL DMEM (Gibco®, ***Life Technologies***), 250 mL M199 (*Sigma-Aldrich*), 5 mL glutamine-PS (100X, Gibco®, **Life Technologies**), 50 mL HS (Horse serum; *Sigma-Aldrich*), 25 mL FBS (Fetal bovine serum; *PAA Laboratories*). Cardiomyocytes remaining in the supernatant were seeded in 12- or 24-well plates coated with 0.1% gelatin (*Sigma-Aldrich*) or in glass bottom Petri dishes coated with laminin (***Life Technologies***). Medium was changed daily until the cells were used.

Isolated adult murine cardiomyocytes were obtained from mouse hearts enzymatically dissociated. C57BL/6J mice were injected intraperitoneally with a single dose of heparine (250 U; Héparine Choay®, 25000 U.I. /5 mL; *Sanofi-Aventis*). Anesthesia was induced 10 min later by injecting a mixture of ketamine (14 mg/kg; Imalgène® 500; *Merial*), xylazine (14 mg/kg; Rompun® 2%; *Bayer*) and pentobarbital (76.6 mg/kg; *Ceva Santé Animale*). The chest was opened and the heart was harvested (leading to the sacrifice of the animal).

Hearts were mounted on a Langendorff apparatus (homemade) and perfused for 15 min with normal Tyrode buffer [140 mM NaCl (*Sigma-Aldrich*), 5.4 mM KCl (*Sigma-Aldrich*), 1 mM $MgCl_2$ (*Sigma-Aldrich*), 5 mM Hepes (*Sigma-Aldrich*), 5.5 mM Glucose (*Sigma-Aldrich*), 147 mM $CaCl_2$ (*Sigma-Aldrich*)]. After stabilization, hearts were subjected to a 30 min global ischemia followed by 60 min of reperfusion (IR protocol) with Tyrode buffer. The peptide treatment (1 µmol/L in Tyrode buffer) was applied at the onset of reperfusion during 1 min. At the end of reperfusion (IR), the heart was perfused with a Ca^{2+}-free Tyrode buffer for 4 min followed by an enzymatic solution of Liberase™ (0.2 mg/mL; *Roche*) for 2-4 min as previously described.[7] Hearts were removed from the apparatus and stored in a "Stop solution" (10 mM 2-3 butanedione monoxime (*Sigma-Aldrich*), 5.5 mM glucose (*Sigma-Aldrich*), 12.5 µM $CaCl_2$ (*Sigma-Aldrich*) and 5% FBS) to block enzymatic digestion. Atria were quickly removed. Single rod-shape myocytes were collected after mechanical dissociation of the ventricles and preplate to remove fibroblasts. Cardiomyocytes were then

plated on coverslips in culture medium contained DMEM (Dulbeco Modified Essential Medium; *Invitrogen*), 20% FBS (*Invitrogen*), 1%-non essential amino acids (*Sigma-Aldrich*), 1%-Insulin-Transferrin-Selenium and 1% Penicillin-Streptomycin solution (*Invitrogen*) at least 2 h before immunohistochemistry.

1.5. Tat-DAXXp treatment on cell cultures

Cellular localization: C2C12 cells or primary neonatal cardiomyocytes were seeded on glass bottom dish (FluoroDish, *World Prescision*) in the appropriate medium (see above). After 24 h, the cells were incubated in OptiMEM (Gibco®; *Life Technologies*) with CF-labeled peptides (1 µM, 1 h or 4 h). Thereafter, they were washed with PBS and co-incubated with Hoechst 33342 dye (blue fluorescence) for 10 min in order to stain nuclei. The distribution of fluorescence in live unfixed cells was analyzed on a Zeiss Axiovert 200 M fluorescence microscope.

Internalization mechanism: C2C12 cells (20,000 cells/well) were seeded in a 24-well plate and grown overnight. The next day, the cells were pre-incubated for 30 min at 4°C or with the different endocytosis inhibitors at the indicated concentrations (in OptiMEM) at 37°C. Afterwards, CF-peptides [1 µmol/L final concentration] were added for an additional 1 h incubation using the same incubation temperature as applied in the pre-incubation. Then, cells were washed 2x in PBS and extracellular membrane-bound peptide were removed by a 10 min incubation with 100 µL 0.05% trypsin (Gibco®; *Life Technologies*) at 37°C, 5% CO_2. Detached cells were transferred in 1.5 mL tubes after addition of 400 µL D-PBS (Gibco®; *Life Technologies*) complemented by 5% FBS (*PAA Laboratories*), followed by centrifugation (10 min, 4°C, 1,500 rpm). Pellets were resuspended in 500 µL D-PBS complemented by 0.5% FBS and 0.1% propidium iodide (PI) (*Molecular Probes*) and cell suspensions were transferred to polystyrene round-bottom tubes (*Falcon*). Fluorescence analysis was performed with a BD

FacsCanto flow cytometer (*BD Biosciences*). Cells stained with PI were excluded from further analysis. A minimum of 10,000 events per sample was analyzed.

The following endocytosis inhibitors were used: nystatin (NYS, 50 µmol/L), chlorpromazine (CPZ, 7.5 µmol/L), 5-(N-ethyl-N-isopropyl)-amiloride (EIPA, 10 µmol/L), sodium azide (NaN_3, 10 mmol/L) and 2-deoxy-glucose (DG, 6 mmol/L) (for ATP depletion) (all from *Sigma-Aldrich*).

1.6. Animal experiments

All experiments were carried out with C57BL/6J mice (*Charles River laboratories*) in accordance with the European Communities Council directive of November 1986 and conformed to the "Guide for the Care and Use of Laboratory Animals" published by the US National Institutes of Health (NIH publication 8th Edition, 2011). The surgical protocols were approved by the “Comité d’Ethique pour l’Expérimentation Animale Languedoc-Roussillon” (CEEA-LR) with the authorization number CE-LR-0814.

1.7. Langendorff ex vivo studies

For *ex vivo* experiments, C57BL/6J male mice were anesthetized with a first intramuscular injection of an anesthetic cocktail comprising ketamine (14 mg/kg, Imalgène®; *Merial*) and xylazine (14 mg/kg, Rompun®; *Bayer*), and by a second injection of pentobarbital (76.6 mg/kg; *Sanofi-Aventis*). Mice were treated (IP injection) with heparin (250U, Héparine Choay®; *Sanofi Aventis*) in order to prevent the blood clot formation. Hearts were excised after sternotomy and cannulated through the ascending aorta. Then, the heart was quickly mounted on the Langendorff system and retrogradely perfused with a pre-warmed Krebs buffer [116 mM NaCl (*Sigma-Aldrich*), 5 mM KCl (*Sigma-Aldrich*), 1.1 mM $MgSO_4$ $7H_2O$ (*Sigma-Aldrich*), 0.35 mM NaH_2PO_4 (*Sigma-Aldrich*), 27 mM $NaHCO_3$ (*Sigma-Aldrich*), 10 mM Glucose (*Sigma-*

Aldrich), 1.8 mM $CaCl_2$ (*Sigma-Aldrich*), pH 7.4, oxygenated with carbogen (95% CO_2, 5% O_2; *Linde*)] at constant pressure and temperature (37°C).

Ischemia-reperfusion protocols

IR was achieved *ex vivo* by either using global ($I_{30}R$) or regional ischemia (IR) models.

- Global ischemia was induced on a homemade Langendorff system by stopping the perfusion during 30 min (no-flow). Reperfusion was achieved by restoring the liquid perfusion during 60 min with the Krebs solution (control) or with peptide solutions administrated during the first minute of reperfusion.

- Regional IR was obtained on an EMKA system (*EMKA Technologies*) allowing coronary blood flow and ECG recordings. The coronary circulation was perfused at 80 mmHg over a 2 to 4 mL/min flow range with an oxygenated Krebs buffer. During the stabilization phase, a 7.0 prolene ligature (*Ethicon*, *Johnson & Johnson*) was placed around the left coronary artery 1-2 mm distal from where it emerges beneath the left atrium and the ends of the ligature were passed through an occluder tube, initially without tension. Heart temperature was continuously assessed by a probe positioned on the base of the heart and recorded by using a TH-5 monitoring thermometer (*Phymep*). Perfused hearts were then immersed in a water-jacketed bath and continuously maintained at 37°C. After a stabilization phase of 20 min (baseline), regional normothermic ischemia was induced by tightening the suture with the occluder tube for 40 min. After ischemia, reperfusion was allowed for 1 h by loosening the ligature. Peptides were perfused during the first minute after the onset of reperfusion, following by a perfusion of 59 min with Krebs buffer. At the end of reperfusion, the artery was reoccluded, the hearts were removed from the perfusion system. For infarct size analysis, hearts were injected with phthalocyanine blue through the aortic cannula and allowed to perfuse the non-ischemic portions of the myocardium, making possible a delineation of the area at risk. For *Western blots* analysis, the hearts were removed from the Langendorff without any blue dye

injection and stored at -80°C until protein extraction. Sham hearts were perfused the same time as those subjected to IR without any coronary ligation.

Recording of the developed tension:

Developed tension was measured on a homemade Langendorff system comprising a transducer connected to the DMT amplifier (*DMT 920 CS*). The transducer position was adjusted using a micromanipulator to give a diastolic tension of 1.0 g. Apicobasal displacement was measured through a small hook attached to the apex of the heart. The recordings were obtained on a PC computer through a digidata and PClamp 9.2. All data were analyzed using Clampfit 9.2 software (*Axon Instruments*).

Recording of coronary blood flow:

During regional *ex vivo* IR protocol, the coronary flow was continuously digitized at 0.1 Hz and recorded using an IOX data acquisition system (*EMKA Technologies*). Excel software (*Microsoft*) was used to perform offline analysis of the recorded data. For each mouse, a mean value of maximal coronary flow was calculated each 10 min. Values during ischemia and reperfusion were normalized with respect to the pre-ischemia phase (baseline) and were expressed in percentages.

Electrocardiographic recordings and analysis:

During regional *ex vivo* IR protocol, ECG was continuously recorded by Ag/AgCl electrodes positioned on the right atrium and near the apex. Signals were digitized continuously at 1 kHz and recorded using an IOX data acquisition system (*EMKA Technologies*). The software ecgAUTO (*EMKA Technologies*) was used to perform offline analysis of the recorded data. For each mouse the mean heart rate (HR) value during baseline, ischemia and reperfusion was calculated.

1.8. Surgical protocol of myocardial ischemia-reperfusion in vivo

Surgical preparation: Acute myocardial ischemia and reperfusion were performed in C57BL/6J mice as previously described.[8] Male mice (22-30 g) were anaesthetized with an intramuscular (IM) injection of an anaesthetic mixture comprising ketamine (50 mg/kg; Imalgène® 500; Merial), xylazine (10 mg/kg; Rompun® 2%; *Bayer*) and chlorpromazine (1.25 mg/kg; Largactil® 5 mg/ml; *Sanofi-Aventis*). Mice were ventilated via a tracheal intubation on a Harvard rodent respirator (tidal volume 7.2 µL/g body mass; respiratory rate 200 breaths per min). The body temperature was maintained constant between 36.8°C and 37.0°C owing to the thermo-regulated surgical table connected to a rectal probe. After a second injection of ketamine (50 mg/kg) and xylazine (10 mg/kg), the chest was opened by a left lateral thoracotomy and a reversible coronary artery snare occluder was placed around the left coronary artery. All animals underwent 40 min of ischemia followed by reperfusion by loosening the knot. When reperfusion lasted 60 min, a third administration of ketamine/xylazine was performed (same dose as in the previous injection, IM). The heart was removed at the end of the surgical protocol.

When reperfusion lasted 24 h, mice underwent a recovery protocol comprising subcutaneous administration of lidocaine (1.5 mg/kg; Xylocain® 10 mg/mL; *AstraZeneca*), and a post-operative awakening in an emergency care unit maintained at 28°C, with oxygen supply and controlled humidity. After 2 h of stabilization, mice were allowed to recover in a ventilated cabinet during 20 h. Mice subjected to 24 h reperfusion were anesthetized again according to the same protocol described for a short period of reperfusion and the heart was removed for infarct size and apoptosis analysis. In SHAM-operated mice (n=3), the suture was passed but not tied and the heart was removed as described before.

In vivo experimental design: Mice were randomly allocated to two different surgical protocols of myocardial IR. **IR 1h**: 40 min ischemia, 1 h reperfusion and **IR 24h**: 40 min ischemia and

24 h reperfusion. All peptides were diluted in physiological saline serum and administered intravenously 5 min before reperfusion or 15, 30 or 45 min after the onset of reperfusion. The control groups were treated with the free Tat peptide (CPP alone), the scrambled version of the peptide (TDS) or with physiological saline serum alone. All peptides were used at the indicated concentrations indicated in the figures legends.

At the end of reperfusion, the artery was re-occluded. The phtalocyanine blue dye (TTC; *Sigma-Aldrich*) was injected into the left ventricle (LV) cavity and allowed to perfuse the non-ischemic portions of the myocardium. Hearts were harvested, atria and right ventricle removed and dedicated to infarct size or DNA fragmentation measurements.

1.9. DNA fragmentation

In vitro assay: Cells were seeded in 24-well plates and grown for 24 h to 48 h (37°C, 5% CO_2). Cells were incubated with staurosporin (STS, 0.1 µmol/L for C2C12 and 1 µmol/L for cardiomyocytes) with or without peptide (in OptiMEM, Gibco®; *Life Technologies*) as described in **Figure 1D and Figure S2**. After apoptosis induction, the solution was replaced by plating medium (250 ml DMEM (Gibco®; ***Life Technologies***), 250 mL M199 (*Sigma-Aldrich*), 5 ml glutamine-PS (100X, Gibco®; ***Life Technologies***), 50 mL HS (Horse serum; *Sigma-Aldrich*), 25 mL FBS (Fetal bovine serum; *PAA Laboratories*) and plates were further incubated for 40 h. DNA fragmentation was quantified on cell lysates with an enzyme-linked immunosorbent assay kit (Cell Death ELISA; *Roche Diagnostics*) designed to quantitate histone-complexed DNA fragments (mono- and oligonucleosomes) in the cytoplasm of cells. DNA fragmentation data were expressed as a "DNA enrichment factor" according to manufacturer's instructions. These values were first normalized to the negative control (condition without STS and peptide) and thereafter related to the STS-condition (corresponding to 100% DNA fragmentation).

In vivo assay: Lysates of transmural samples of non-ischemic (NI) or ischemic (I) areas of the left ventricles were prepared as previously described.[9] In both cases, DNA fragmentation was quantified with an enzyme-linked immunosorbent assay kit as described in the previous section. Transmural samples from 30 mg of non-ischemic areas of the left ventricle (central portion of the septum) and ischemic areas (portion of the LV free wall directly under the silk ligation) were harvested on mice submitted to the surgical protocol. Tissues samples were disintegrated in a tissue grinder in 400 µL of the lysis buffer supplied with the kit. The homogenate was centrifuged at 13,000 g for 10 min. The supernatant was used as antigen source in the sandwich ELISA. Incubation buffer, instead of the sample solution, and DNA-histone complex were used as negative and positive controls, respectively. Two values from the double absorbance measurements (405 nm / 490 nm) of the samples were averaged, and the background (negative control) was subtracted from each of these averages. The positive control was used as an internal control for daily variability. DNA soluble nucleosomes were quantified both in blue-colored region (non-ischemic region = NI) as well as in the non blue-colored areas (ischemic region = I). This allows to normalize the rate of DNA fragmentation (internal control) and to avoid the introduction of variability in the results due to differences in temperature, timing of the measurement.

1.10. Infarct size assessment

LV were sliced transversally into 1-mm-thick sections and incubated in a 1% solution of 2,3,5-triphenyltetrazolium chloride (TTC, *Sigma-Aldrich*) for 15 min at 37°C. After fixation in a 4% paraformaldehyde–PBS solution, the slices were weighted and each side was photographed (*Olympus* camera). The ischemic risk area and the infarcted area were measured by planimetry with ImageJ software (*U. S. National Institutes of Health*). Infarct size was expressed as a percentage of the ischemic risk area.

1.11. Immunoblotting

Tissue samples (left ventricle) were rapidly frozen in liquid nitrogen after the end of *ex vivo* IR protocols. Samples were homogenized with a grinder in RIPA buffer [50 mM Tris (*Sigma-Aldrich*), 150 mM NaCl (*Sigma-Aldrich*), 1% Triton X-100 (*Sigma-Aldrich*), 0.1% sodium dodecyl sulfate (*Sigma-Aldrich*) pH 8.0] supplemented with EDTA-free protease and phosphatase inhibitor (Halt™ Protease and phosphatase single-use inhibitor Cocktail-100X, *Thermoscientific*). After centrifugation, pellets were resuspended in RIPA buffer for protein purification and incubated for 1 h at 4°C. Protein concentrations were determined with the bicinchoninic acid (BCA) protein assay kit (*Pierce*). Samples (25 µg) of protein were resolved by SDS polyacrylamide gel electrophoresis (4-20% mini-Protean®TGX™ precast gels; *Biorad*) and transferred to nitrocellulose (Trans-Blot®Turbo™; *Biorad*). The following antibodies and suppliers were used: 1) *EMD Millipore*: anti-caspase 3 (Upstate 06-735), 2) *Cell Signaling Technology:* anti-phospho ERK1,2; anti-ERK1,2; anti-phospho JNK1,2; anti-JNK1/2; anti-phospho AKT; anti-AKT; cleaved caspase-8 (ASP387)(D5B2); RIP1 (D94C12); RIP3 (D8J3L); caspase 9; Beclin-1 (D40C5); LC3A/B (D3U4C); β-Tubulin; anti-α-actinin; vinculin (E1E9V), GAPDH, 3) *Abcam:* FAS, DAXX (M-112), anti-phosphoMLKL (phosphoS345), FADD (EPR5030), HSP70, BAD (Y208), 4) *Biorbyt Ltd:* phosphoDAXX and 5) *Jackson ImmunoResearch:* horseradish peroxidase-conjugated anti-rabbit. Protein bands were visualized by enhanced chemiluminescence method using an ECL kit (SuperSignal™ West Pico chemiluminescent Substrate; *Thermo Scientific*™). Densitometry analysis was performed using Chemidoc™ (*Biorad*) and ImageJ software (*U. S. National Institutes of Health*). Signal intensities of each protein band were corrected with the corresponding value obtained for the loading controls (tubulin, vinculin, GAPDH or α-actinin) and then normalized with the mean value obtained for the IR control conditions.

1.12. Immunostaining

Cultured ventricular myocytes were fixed in 4%-paraformaldehyde (in PBS solution) and co-incubated 2 h at room temperature using anti-DAXX primary antibody (sc-7152; *Santa Cruz Biotechnologies*).

After primary antibody incubation, cells were washed in PBS, and then incubated (1 h at room temperature) with the secondary antibody (1:2000; *Jackson ImmunoResearch*). Cell nuclei were stained with DAPI (*Sigma-Aldrich*). Coverslips were mounted in Citifluor™ (*Biovalley*) and slides were imaged with a microscope (40x oil objective).

1.13. SPECT-CT imaging

C57BL/6J (male, 6–8 weeks old) were force-fed with Lugol solution one day before imaging, and stable iodine was added to their drinking water for the entire experimental period.

Mice were anesthetized with 2% isoflurane and positioned on the head of 4-head multiplexing multipinhole NanoSPECT camera (*Bioscan Inc*.). Whole-body SPECT/CT images were acquired at various times (0, 3, 6, and 24 h) after tail vein injection of 10 MBq radiolabeled ^{125}I-TD in control mice or at the time of reperfusion in IR mice.

Energy window was centered at 28 keV with ±20% width. Acquisition times were defined to obtain 30,000 counts for each projection with 24 projections. Images and maximum intensity projections (MIPs) were reconstructed using the dedicated Invivoscope® (*Bioscan Inc*.) and Mediso InterViewXP® software (*Mediso Medical Imaging System*). Concurrent microCT whole-body images were performed for anatomic co-registration with SPECT data. Reconstructed data from SPECT and CT were visualized and co-registered using Invivoscope®.

1.14. Statistical analysis

All values are expressed as mean ± SD. Statistical analysis was performed only for $n \geq 5$ independent experiments. Data were analyzed with nonparametric Kruskal-Wallis test for multiple comparison or Mann-Whitney when appropriate. For repeated measures, data were analyzed with Two-way RM ANOVA and the Tukey's or Sidak's post-test. Concerning **Figures 6B and C**, infarct size data (mean ± SD) were fitted by a linear regression model using the least squares method based on the minimization of the sum of squares of the vertical distances of the points from the line. Values of $P<0.05$ were accepted as statistically significant. P values, indicated in the text, were noted in the figures as * for $p<0.05$, ** for $p<0.01$, *** for $p<0.001$ and **** for $P<0.0001$. Data were analyzed with GraphPad Prism (*GraphPad Software*).

2. Supplemental Results

2.1. Screening of DAXXp interfering peptides

A peptide library of 15-mer overlapping peptides (PepScan array) spending the entire primary sequence of the human DAXX was screened with the intracellular region of the FAS receptor (FasR) as outlined in **Figure S1A**. The highest signal intensities were measured for peptides 209 to 212 on the array (**Figure S1B**). Since this set of peptides is included in the DAXX-DN (dominant-negative) construct found to be cardioprotective in our previous studies,[8] we focused on this region to design a cardioprotective peptide.

2.2. Determination of the optimal anti-apoptotic DAXXp peptide

The interfering peptide (DAXXp) was coupled to the Tat cell penetrating peptide for the cellular internalization resulting in the Tat-DAXXp (TD). First, we analyzed the cell viability on the C2C12 model cell line by incubating them with TD in a dose-dependent manner (**Figure S2A**). No toxic effect could be detected using concentrations between 0.5 µmol/L and 2.5 µmol/L of TD after 24 h incubation, which is an important prerequisite in the development of a therapeutic drug development (p=ns *versus* untreated).

More importantly, the anti-apoptotic activity of TD was then evaluated in C2C12 cells submitted to a staurosporin (STS)-induced apoptotic stress (0.1 µmol/L; see protocol in **Figure S2B**) followed by specific DNA fragmentation quantification (**Figure S2C**). A 23%-decrease in DNA fragmentation was observed in cells treated with 1 µmol/L TD ($p<0.05$ *versus* Tat). As a control, we also evaluated the murine peptide sequence (Tat-mDAXXp) and determined exactly the same 23%-reduction of DNA fragmentation ($p<0.05$ *versus* Tat) confirming the homology of both DAXX sequences. Neither the Tat delivery vector alone nor a scrambled version of the peptidic inhibitor (TDS) were able to inhibit apoptosis. As expected from its poor

in vitro uptake, the free DAXXp did not induce any anti-apoptotic activity even at a 10 µmol/L concentration.

2.3. Evaluation of Tat-DAXXp trafficking in vitro

The sub-cellular localization of a carboxy-fluorescein (CF)-labelled TD revealed a punctuated cytosolic pattern after 1 h incubation in C2C12 cells (**Figure S3A**, left panel). This indicates, that TD is probably internalized via an endocytotic pathway. However, after a prolonged incubation time (4 h), TD seems to escape from the endosomal vesicles as shown by a more diffuse peptide pattern in the cytosol (**Figure S3A**, right panel).

To determine which endocytotic pathways are involved in the trafficking of TD in C2C12 cells, we took advantage of pharmacological inhibitors of the major endocytic pathways. C2C12 cells were treated with chlorpromazine (CPZ) for clathrin-mediated endocytosis inhibition, with nystatin (Nys) for caveolae-mediated endocytosis inhibition or with 5-(N-ethyl-N-isopropyl) amiloride (EIPA) for macropinocytosis inhibition. Furthermore, cells were incubated at 4°C for membrane fluidity reduction or with NaN_3 and 2'-Deoxy-D-Glucose (DDG) for ATP-depletion (-ATP). Fluorescence spectroscopy analysis showed that the peptide is mainly internalized *via* an energy- and clathrin-dependent pathway as shown by a significant uptake reduction using the 4°C (-74%) and the ATP depletion (-63%) conditions as well as with chloropromazin (-57%) (**Figure S3B**).

2.4. Determination of the optimal DAXXp length

The minimal active sequence (MAS) of the interfering peptide was investigated first by synthesizing the peptides corresponding to sequences 209 to 212 issued from PepScan screening (**Figure S1B**) to confirm that the TD sequence has the highest anti-apoptotic effect as revealed by the DNA fragmentation assay (**Figure S4A**). Thereafter, length analyses were

performed based on the 18-mer variants 209-210 and 211-212 by cutting the respective sequences from the N-terminus or the C-terminus (**Figure S4B**). The highest signal intensities were observed with spot #6 (= sequence 211) and spot #27 (= sequence 209), showing that the peptide could not be elongated or shortened. This was further confirmed with several shorter TD variants (15-, 14-, 13 and 9-mer) having no or significant less anti-apoptotic effect compared to TD as observed by DNA fragmentation quantification (**Figure S4C**).

Altogether, we could define the minimal active sequence issued from the human DAXX protein as the 16-mer DAXXp sequences, which was therefore used coupled to the Tat vector in all further experiments.

2.5. Time-dependent level of phospho-DAXX during myocardial IR.

As reported in our previous work, the time window of cardioprotection offered by postconditioning in mice subjected to IR injury may be larger than initially reported.[10] In this study, we show that postconditioning when applied at 10 seconds or 1, 5, 10, 15, or 30 minutes after the onset of reperfusion reduced infarct size and DNA fragmentation.

This delayed time window of 15 to 30 min was also observed for the TD administration after the onset of reperfusion (**Figure 6**). TD cardioprotection is effective even if the DAXX protein is phosphorylated 15 min after reperfusion (**Figure S9**). The amount of phosphorylation reached 63% of that obtained in the non-treated IR_{60} condition. If we consider the corresponding apoptosis rates evaluated *in vivo* in the hearts subjected to the same injury (40 min ischemia-15 min reperfusion), we evidenced that in the IR_{15} group, specific DNA fragmentation level represents at this time only 43% of the value obtained for IR (maximal level; for details, see[10]). These results confirm that DAXX phosphorylation is an early mechanism upstream the rise in apoptosis that occurs later reaching a plateau at 60 min. In addition, we evidenced an efficient cardioprotection for $TD_{\Delta 15}$ *versus* Tat when the peptide was administered 15 minutes after the

onset of reperfusion (see **Figures 6B and C**) with a 42%-decrease in both infarct size and the release of soluble nucleosomes (specific DNA fragmentation) ($TD_{\Delta 15}$ *versus* Tat, p*; see **Figures 6B and D**). This suggests that DAXX nucleo-cytoplasmic export, as a consequence of DAXX phosphorylation, happens during the first minutes of the wave front of IR injury and that the strong inhibition of apoptosis due to the TD administration happens even if DAXX is exported from the nucleus. In sum, TD cardioprotection occurs even if DAXX protein is phosphorylated and probably exported to the cytoplasm.

2.6. Indirect role of Tat-DAXX on the DAXX nuclear export.

Previous studies have shown that DAXX protein, which contains two nuclear localization signals, is mainly located in the nucleus of unstressed cells[11]. DAXX nucleocytoplasmic export is triggered by oxidative stress in cardiac cells[12, 13] or by glucose deprivation[14]. Upon stress, DAXX phosphorylation (Serine 667) results in conformational changes exposing the nuclear export signal (NES), which is recognized by the chromosomal region maintenance 1 receptor (CRM1 or exportin 1).[15, 16] The CRM1 is a carrier protein and a receptor recognizing the NES of DAXX protein having the following amino acid sequence: LFELEIEALPL (565–575 AA sequence of the DAXX protein). TD peptide (625-637 AA sequence of the DAXX protein) is not issued from the NES region, is not homologue to this NES region and more importantly did not contain the serine 667. For all mentioned reasons, we estimate that TD peptide could not act as a bait on CRM1 receptor in order to block DAXX nuclear export.

ASK1 (Apoptosis signal-regulating kinase 1) is also a DAXX-interacting protein that insures shuttle DAXX-shuttling during nucleo-cytoplasmic transport into the cytoplasm.[17] Because ASK1 binds to the DAXX protein by interaction with the region spanning sequence from amino acid 501 to 625[14], we exclude the possibility that TD interacts with ASK1 (so no change in the feedback loop controlling DAXX nucleo-cytoplasmic export).

In conclusion, if DAXX nucleo-cytoplasmic transport depends on specific interactions between first DAXX and CRM1 and second DAXX and ASK1 after DAXX nuclear export, there is no chance for the TD peptide to interact with these two proteins instead of DAXX, leading to a direct impact of TD on the nucleo-cytoplasmic export.

Altogether these data suggest that DAXX nuclear trafficking may be indirectly influenced by the TD treatment as a result of its impact on both apoptotic and survival pathways as well as on the feedback loops controlling DAXX nucleo-cytoplasmic ratio (**Figure 7**).

3. Supplemental Tables

Table S1: Peptide sequences.

Peptide	Sequence	AA
Tat	GRKKRRQRRRPPQ	13
Tat-DAXXp (TD)	GRKKRRQRRRPPQ-KKSRKEKKQTGSGPLG	29
Tat-scrDAXXp (TDS)	GRKKRRQRRRPPQ-KKGRKQSGESLGTPKK	29
Tat-DAXXp-209	GRKKRRQRRRPPQ-SGPPCKKSRKEKKQT	28
Tat-DAXXp-210	GRKKRRQRRRPPQ-PCKKSRKEKKQTGSG	28
Tat-DAXXp-211	GRKKRRQRRRPPQ-KSRKEKKQTGSGPLG	28
Tat-DAXXp-212	GRKKRRQRRRPPQ-KEKKQTGSGPLG	28
Tat-DAXXp-14	GRKKRRQRRRPPQ-SRKEKKQTGSGPLG	27
Tat-DAXXp-13	GRKKRRQRRRPPQ-RKEKKQTGSGPLG	26
Tat-DAXXp-9	GRKKRRQRRRPPQ-KSRKEKKQT	22

Footnote: Tat-DAXXp-211 correspond to Tat-DAXXp-15 in Figure S4C

Table S2: Summary of the *in vivo* results.

Conditions	Peptides	Dose (mg/kg)	Infarct size (% of AR) [n]	Area at risk (% of LV) [n]	Soluble nucleosomes (ratio I/NI) [n]
40 min I / 1 h R	Tat	1	38.37 ± 8.46 [14]	43.42 ± 5.74 [14]	4.09 ± 0.75 [11]
	TD	0.1	30.85 ± 6.34 [6]	46.19 ± 3.65 [6]	3.30 ± 1.37 [11]
	TD	1	15.54 ± 6.90 [11]	45.47 ± 5.18 [11]	1.61 ± 0.44 [6]
	TD	10	16.02 ± 3.84 [6]	43.06 ± 5.84 [6]	1.29 ± 0.45 [6]
	TDS	1	35.64 ± 6.28 [6]	46.66 ± 4.76 [6]	3.92 ± 1.19 [7]
	$TD_{\Delta15}$	1	21.97 ± 0.95 [6]	46.12 ± 4.90 [6]	2.38 ± 0.27 [6]
	$TD_{\Delta30}$	1	25.12 ± 4.95 [10]	44.92 ± 5.05 [10]	2.58 ± 0.51 [11]
	$TD_{\Delta45}$	1	36.80 ± 7.15 [9]	43.95 ± 5.06 [9]	4.17 ± 0.35 [8]
40 min I / 24 h R	Tat	1	33.29 ± 6.07 [17]	44.41 ± 4.99 [17]	4.01 ± 1.34 [13]
	TD	0.1	22.41 ± 6.15 [7]	46.48 ± 5.20 [7]	2.17 ± 0.43 [6]
	TD	1	17.10 ± 5.16 [8]	41.99 ± 4.57 [8]	1.57 ± 0.37 [6]
	TD	10	13.73 ± 4.79 [6]	46.07 ± 3.41 [6]	1.49 ± 0.60 [6]
	TDS	1	32.84 ± 4.01 [6]	45.18 ± 5.20 [6]	3.37 ± 0.94 [10]
	$TD_{\Delta15}$		19.70 ± 3.87 [6]	45.34 ± 3.49 [6]	1.59 ± 0.29 [6]
	$TD_{\Delta30}$	1	23.62 ± 4.69 [14]	47.13 ± 3.82 [14]	2.34 ± 0.72 [10]
	$TD_{\Delta45}$	1	36.26 ± 6.03 [9]	44.06 ± 7.23 [9]	3.52 ± 0.63 [8]

Footnote: numbers in square brackets represent the number of treated animals.

4. Supplemental Figures

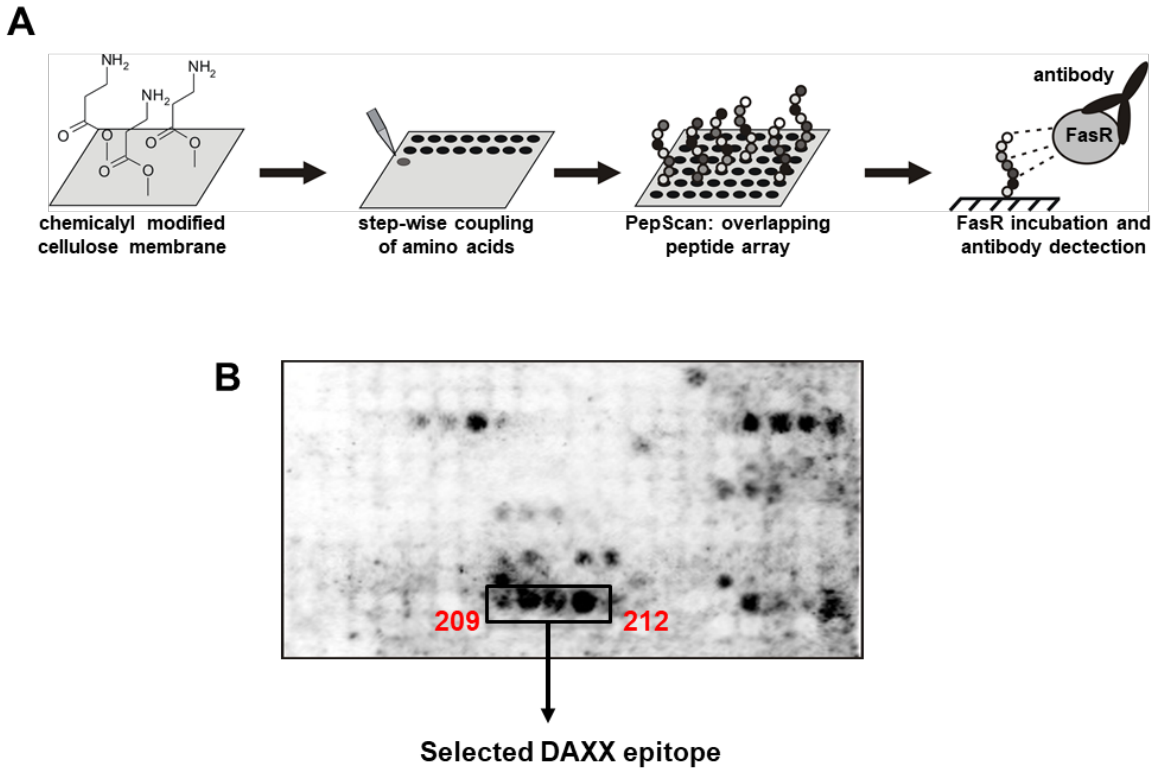

Supplemental Figure S1 : Screening of the DAXX epitope by SPOT synthesis.

(**A**) Principle of the SPOT synthesis: after the amino functionalization of the cellulose membrane, the amino acids were spotted step-wise according to the standard SPOT synthesis.[2] The peptide library was then incubated with the intracellular region of the Fas receptor (FasR) and the interactions were revealed by antibody detection.

(**B**) Peptide library screening: The primary amino acid sequence of the DAXX protein was dissected in overlapping peptides, which were synthesized as an array (PepScan; 15-mer peptides with a 3 amino acids shift). The peptide array was probed for FAS interaction and analyzed in enzyme-linked blot. The black rectangle shows the brightest spots with the corresponding epitope sequence.

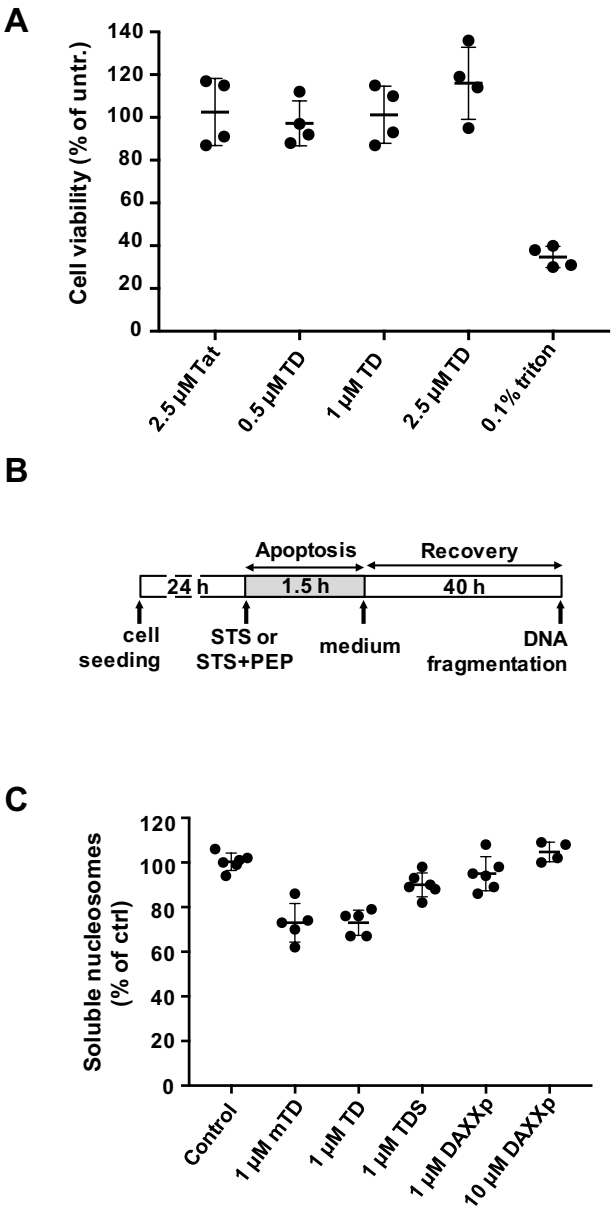

Supplemental Figure S2: *In vitro* evaluation of Tat-DAXXp in C2C12 cells.

(**A**) Cell viability: C2C12 were incubated with increasing concentrations of TD for colorimetric assessment of the cell viability. Data shown are the means ± SD, with n=4 independent experiments. (**B**) Treatment: C2C12 cells were subjected to 0.1 µmol/L staurosporine (STS) for 1.5 h, with or without additional peptide treatment, and followed by 40 h recovery after medium replacement. (**C**) Anti-apoptotic effect: Quantification of DNA fragmentation in C2C12 cells treated by STS and anti-apoptotic peptides (1 µmol/L). Note a 22%-decrease in DNA fragmentation with the murine mTD (for Tat-mDAXXp) as well as with the human TD sequence (1 µmol/L each). Data were normalized relative to control value (STS alone). Data shown are the scatter dot blots and the means ± SD, with n≥ 4 independent cultures.

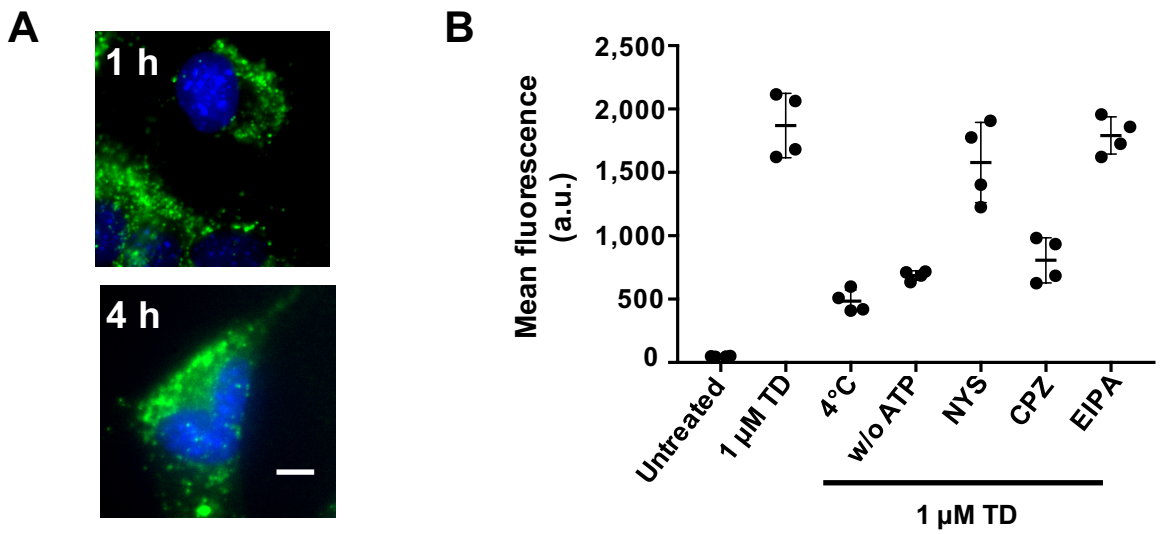

Supplemental Figure S3: Mechanism of cellular internalization of Tat-DAXXp in C2C12 cells.

(**A**) Cellular localization: Representative images of C2C12 cells, which were incubated with 1 µmol/L CF-labeled TD incubated for 1 h or 4 h. Cell nuclei were stained with Hoechst-dye (blue). Bar scale = 10 µm. Original magnification: x63 oil immersion.

(**B**) Trafficking mechanism: C2C12 were incubated with carboxyfluorescence (CF)-labeled TD (1 µmol/L) for 1 h and uptake analyze d by flow cytometry. Untreated cells represent the negative control. To evaluate the internalization pathway, cells were pre-treated 30 min in the following conditions: 4°C, ATP-depletion (w/o ATP: 10 mM NaN_3 + 6 mM DDG), chlorpromazine (CPZ: 7.5 µmol/L), nystatin (NYS: 50 µmol/L), 5-(N-ethyl-N-isopropyl) amilorid (EIPA: 10 µmol/L). Data shown are scatter dot blots and mean ± SD, with n=4 independent experiments.

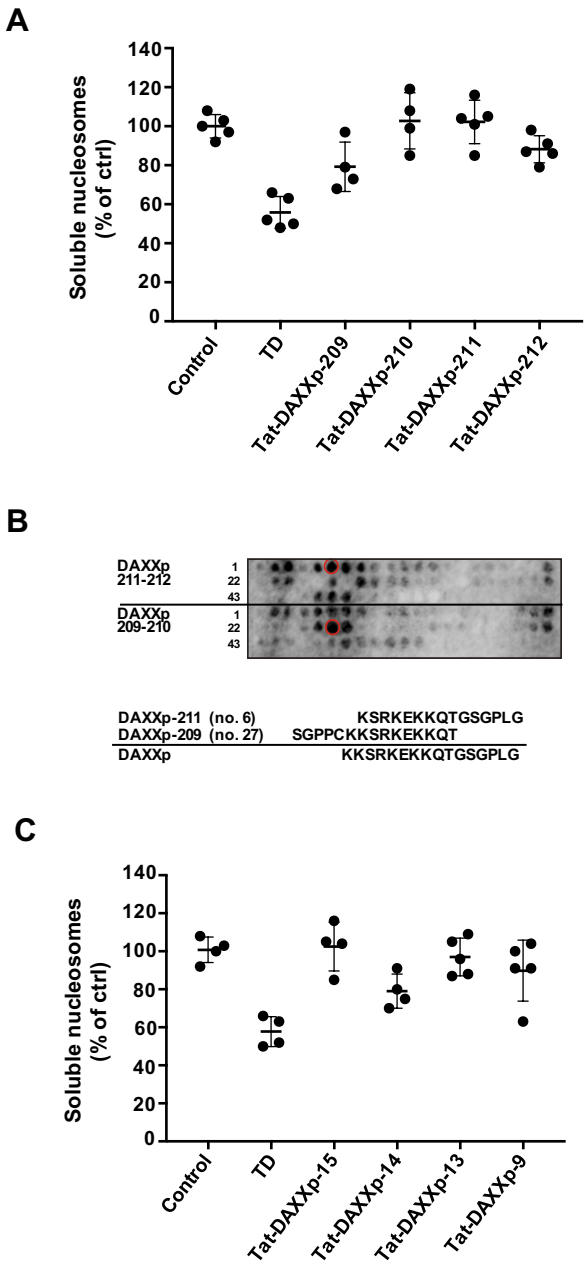

Supplemental Figure S4: Determination of the optimal Tat-DAXXp sequence.

(**A**) Evaluation of the anti-apoptotic activity of TD variants in primary cardiomyocytes using DNA fragmentation. Data are normalized to 100% STS. Data shown are scatter dot blots and means ± SD, with n≥ 4 independent experiments. (**B**) The DAXXp-211 and DAXXp-209 peptides were successively shortened by one amino acid residue at the N-terminus, at the C-terminus or both at the N- and the C-termini, and analyzed using enzyme-linked blot. The spots indicated by a red circle exhibited the highest signal intensities (BLU). (**C**) Evaluation of the anti-apoptotic activity of shorter TD variants in primary cardiomyocytes using DNA fragmentation. Data are normalized to 100% STS. Data shown are scatter dot blots and the means ± SD, with n≥4 independent experiments.

A

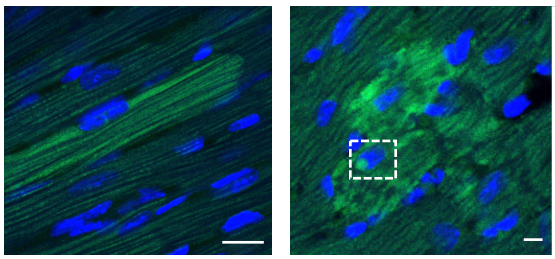

B

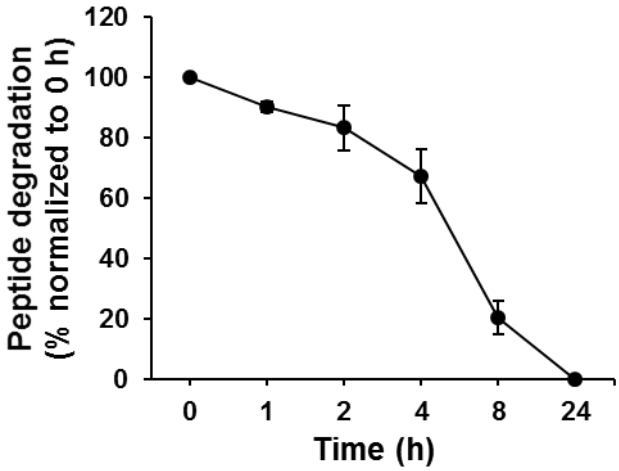

Supplemental Figure S5: Behavior of Tat-DAXXp *in vivo* and *in vitro*.

(**A**): Representative confocal images from LV slices of mice hearts subjected *in vivo* to myocardial IR and injected with CF-TD showing cytoplasmic localization of the peptide (green) and few nuclear localization (DAPI in blue). Bar scales = 50 µm (left), 10 µm (right); (B) Stability of TD was measured in 20% mouse adult serum (37°C) and peptide degradation was analyzed by reverse-phase HPLC (measurement of the peak area in µV*sec) after 0 h, 1 h, 2 h, 4 h, 8 h and 24 h incubation. n = 3.

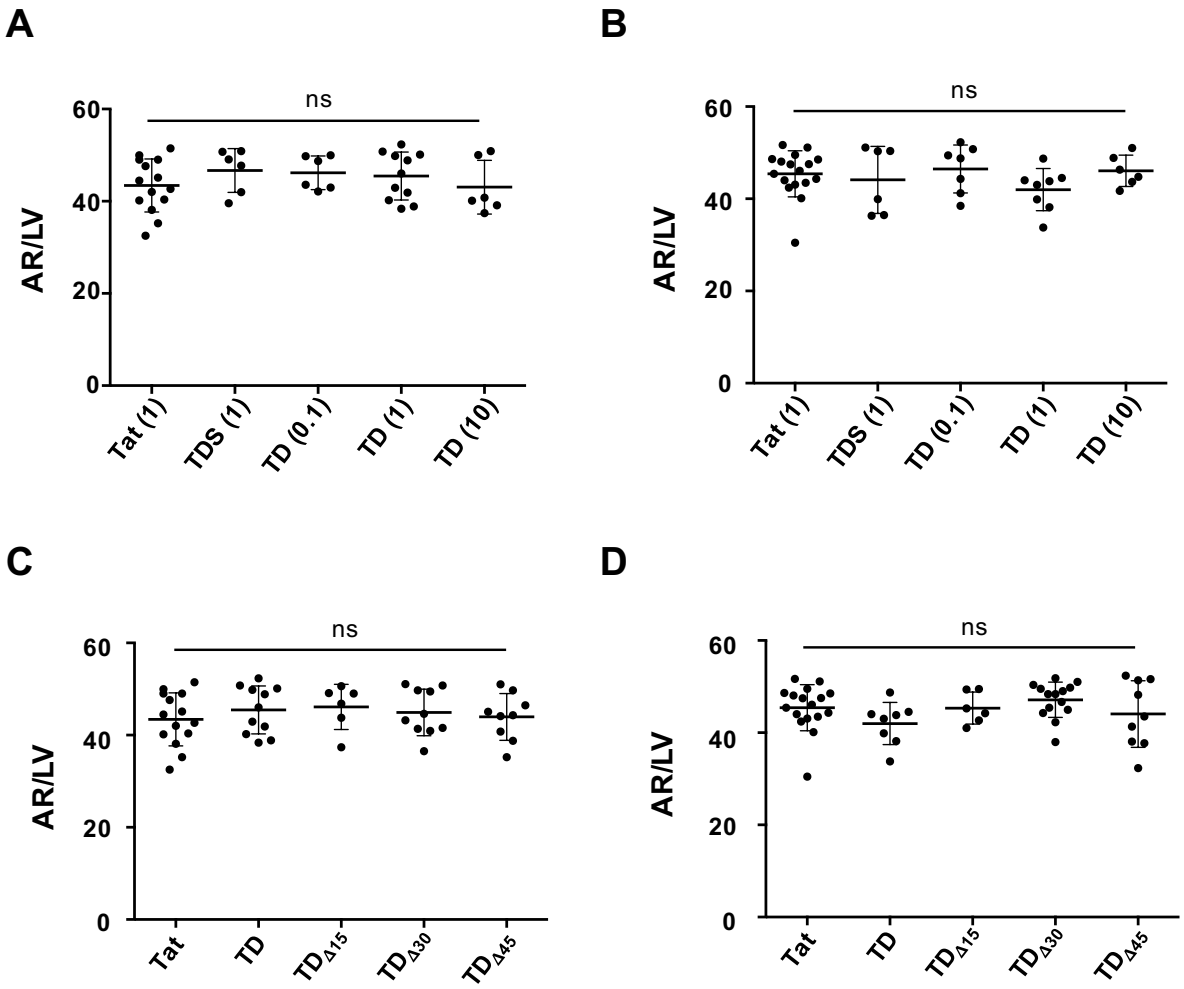

Supplemental Figure S6: Area at risk measured in the study groups of mice subjected to IR.

Area at risk expressed in % of LV mass (AR/LV) was quantified in mice subjected to 40 min-ischemia followed by 1 h (**A, C**) or 24 h of reperfusion (**B, D**). (**A, B**): Scatter dot blots and means ± S.D were plotted for Tat (1 mg/kg), TD (0.1, 1 and 10 mg/kg) or TDS (1 mg/kg) injected intravenously 5 min before reperfusion. (**C, D**): Scatter dot blots and means ± S.D were plotted for all peptides (1 mg/kg) injected 5 min before reperfusion (TD) or for the delayed administration at 15 min ($TD_{\Delta 15}$), 30 min ($TD_{\Delta 30}$), and 45 min ($TD_{\Delta 45}$) after the onset of reperfusion. Statistical significance compared to Tat is noted ns for $p>0.05$. n values are reported in Table S2.

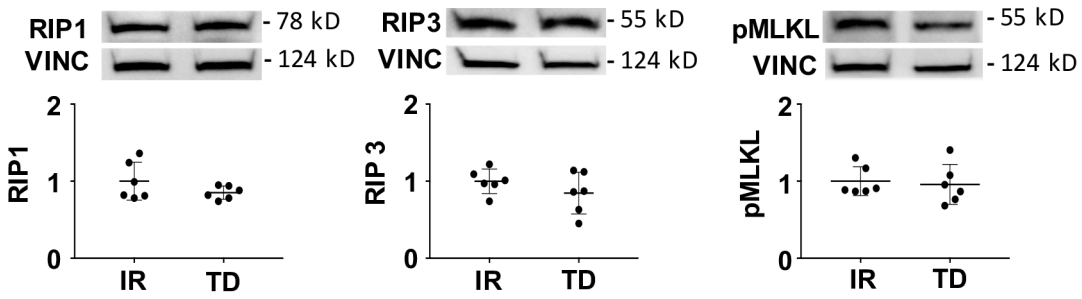

Supplemental Figure S7: Effects of Tat-DAXXp treatment on necroptosis.

Western blot analysis was performed on LV protein extracts. Scatter dot blots and mean ± SD were plotted for RIP1 (p=0.3723), RIP3 (p=0.3939) and pMLKL (p=0.5887) tested in TD (n=6) *versus* IR (n=6) protein extracts. Representative gel blots are presented for each protein. Vinculin (VINC) was used as protein loading control. Statistical analysis was performed using non-parametric Mann-Whitney test revealing no significant difference between groups.

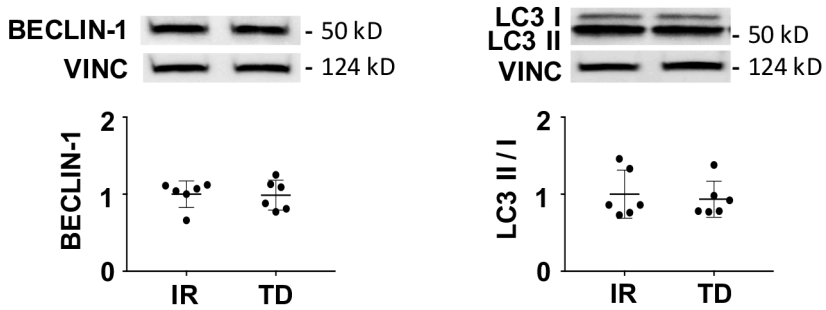

Supplemental Figure S8: Effects of Tat-DAXXp treatment on autophagy flux.

Western blot analysis was performed on LV protein extracts. Scatter dot blots and mean ± SD were plotted for Beclin-1 (p=0.9372) and LC3 II/I ratio (p=0.8939) tested in protein extracts from TD (n=6) *versus* IR (n=6) hearts. Representative gel blots are presented for each protein. Vinculin (VINC) was used as protein loading control. Statistical analysis was performed using non-parametric Mann-Whitney test revealing no significant difference between groups.

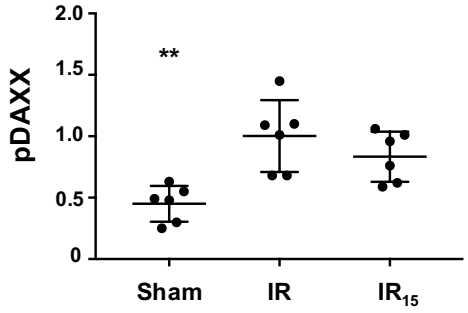

Supplemental Figure S9: Effects of Tat-DAXXp treatment on DAXX phosphorylation.

Western blot analysis was performed on LV protein extracts. Scatter dot blots and mean ± SD were plotted for pDAXX protein tested in Sham (n=6), IR (n=6) and IR $_{\Delta 15}$ (n=6) protein extracts. Representative gel blots are presented for each protein. GAPDH was used as protein loading control. Statistical analysis was performed using non-parametric Kruskal-Wallis followed by the Dunn's post test. Statistical significance was noted p** = 0.0032 for Sham *versus* IR.

5. Supplemental references

1. Bhargava S, Licha K, Knaute T, Ebert B, Becker A, Grotzinger C, Hessenius C, Wiedenmann B, Schneider-Mergener J, Volkmer-Engert R. A complete substitutional analysis of VIP for better tumor imaging properties. *J Mol Recognit* 2002;**15**:145-153.
2. Frank R. Spot synthesis an easy technique for positionally addressable, parallel chemical synthesis on a membrane support. *Tetrahedron* 1992;**48**:9217-9232.
3. Fischer R, Mader O, Jung G, Brock R. Extending the applicability of carboxyfluorescein in solid-phase synthesis. *Bioconjug Chem* 2003;**14**:653-660.
4. Santoro L, Boutaleb S, Garambois V, Bascoul-Mollevi C, Boudousq V, Kotzki PO, Pelegrin M, Navarro-Teulon I, Pelegrin A, Pouget JP. Noninternalizing monoclonal antibodies are suitable candidates for 125I radioimmunotherapy of small-volume peritoneal carcinomatosis. *J Nucl Med* 2009;**50**:2033-2041.
5. Barrere-Lemaire S, Combes N, Sportouch-Dukhan C, Richard S, Nargeot J, Piot C. Morphine mimics the antiapoptotic effect of preconditioning via an Ins(1,4,5)P3 signaling pathway in rat ventricular myocytes. *Am J Physiol Heart Circ Physiol* 2005;**288**:H83-88.
6. Sadoshima J, Izumo S. Molecular characterization of angiotensin II--induced hypertrophy of cardiac myocytes and hyperplasia of cardiac fibroblasts. Critical role of the AT1 receptor subtype. *Circ Res* 1993;**73**:413-423.

7. Vincent A, Sportouch C, Covinhes A, Barrere C, Gallot L, Delgado-Betancourt V, Lattuca B, Solecki K, Boisguerin P, Piot C, Nargeot J, Barrere-Lemaire S. Cardiac mGluR1 metabotropic receptors in cardioprotection. *Cardiovasc Res* 2017;**113**:644-655.
8. Roubille F, Combes S, Leal-Sanchez J, Barrere C, Cransac F, Sportouch-Dukhan C, Gahide G, Serre I, Kupfer E, Richard S, Hueber AO, Nargeot J, Piot C, Barrere-Lemaire S. Myocardial expression of a dominant-negative form of Daxx decreases infarct size and attenuates apoptosis in an in vivo mouse model of ischemia/reperfusion injury. *Circulation* 2007;**116**:2709-2717.
9. Piot CA, Padmanaban D, Ursell PC, Sievers RE, Wolfe CL. Ischemic preconditioning decreases apoptosis in rat hearts in vivo. *Circulation* 1997;**96**:1598-1604.
10. Roubille F, Franck-Miclo A, Covinhes A, Lafont C, Cransac F, Combes S, Vincent A, Fontanaud P, Sportouch-Dukhan C, Redt-Clouet C, Nargeot J, Piot C, Barrere-Lemaire S. Delayed postconditioning in the mouse heart in vivo. *Circulation* 2011;**124**:1330-1336.
11. Ko YG, Kang YS, Park H, Seol W, Kim J, Kim T, Park HS, Choi EJ, Kim S. Apoptosis signal-regulating kinase 1 controls the proapoptotic function of death-associated protein (Daxx) in the cytoplasm. *J Biol Chem* 2001;**276**:39103-39106.
12. Jung YS, Kim HY, Lee YJ, Kim E. Subcellular localization of Daxx determines its opposing functions in ischemic cell death. *FEBS Lett* 2007;**581**:843-852.
13. Yaniv G, Shilkrut M, Lotan R, Berke G, Larisch S, Binah O. Hypoxia predisposes neonatal rat ventricular myocytes to apoptosis induced by activation of the Fas (CD95/Apo-1) receptor: Fas activation and apoptosis in hypoxic myocytes. *Cardiovasc Res* 2002;**54**:611-623.
14. Song JJ, Lee YJ. Role of the ASK1-SEK1-JNK1-HIPK1 signal in Daxx trafficking and ASK1 oligomerization. *J Biol Chem* 2003;**278**:47245-47252.
15. Song JJ, Lee YJ. Catalase, but not MnSOD, inhibits glucose deprivation-activated ASK1-MEK-MAPK signal transduction pathway and prevents relocalization of Daxx: hydrogen peroxide as a major second messenger of metabolic oxidative stress. *J Cell Biochem* 2003;**90**:304-314.
16. Song JJ, Lee YJ. Daxx deletion mutant (amino acids 501-625)-induced apoptosis occurs through the JNK/p38-Bax-dependent mitochondrial pathway. *J Cell Biochem* 2004;**92**:1257-1270.
17. Chang HY, Nishitoh H, Yang X, Ichijo H, Baltimore D. Activation of apoptosis signal-regulating kinase 1 (ASK1) by the adapter protein Daxx. *Science* 1998;**281**:1860-1863.